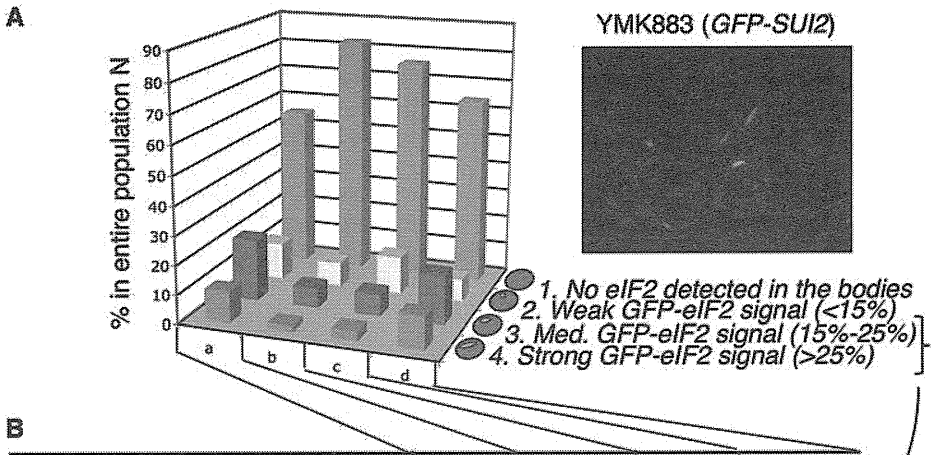

B

Plasmid	Vec	hc yeIF5	5MP1	5MP1-7A
# of cells (N)	255	258	213	232
% of cells with med-strong signal	32%	8.9%	10.8%	28%
Ave. GFP-eIF2 intensity in the body	9.23%	2.74%	3.96%	7.87%
(Standard error)	(0.74%)	(0.42%)	(0.54%)	(0.77%)

Figure 6. Effect of 5MP1 on GFP-eIF2 association with eIF2B bodies. (A) Inset shows a typical image of yeast YMK883 cell expressing GFP-eIF2, with its localization in large cytoplasmic eIF2B bodies (34). YMK883 transformants carrying an empty vector (Vec, column a), YEpL-TIF5-FL (hc yeIF5, column b), pEMBL-FL-5MP1 (5MP1, column c) and pEMBL-FL-5MP1-7A (5MP1-7A, column d) (Supplementary Table S1) were grown in SCGal-ura medium to a mid-log phase. Then, fluorescent images of the cells were taken under a confocal microscope, and quantified for the amount of GFP-eIF2 signal localized in the bodies compared to one in the whole cell. Graph indicates the proportions of the groups of cells (in each column) with no, weak, medium and strong GFP-eIF2 signals in the bodies, as defined in each row of the graph. (**B**) Table summarizing the plasmid used (Row 1), the number of transformed cells measured (Row 2), percentage of cells with med to strong GFP-eIF2 signals in the body (the sum of percentage values in Rows 3 and 4 of graph in A) (Row 3), and percentage of GFP-eIF2 signals localized in the bodies, averaged for the entire population of the cells carrying the same plasmid (Row 4), together with its standard error of the mean ($SD/n^{1/2}$; Row 5).

measurement of both cell growth and the expression of a Gcn4p transcriptional target (*HIS4*) during histidine starvation conditions induced by the inhibitor 3-aminotriazole (3AT). As shown in Figure 7A, Row 1, the growth of a *gcn2Δ* strain is sensitive to 3AT because the absence of eIF2 phosphorylation prevents the preferential translation of *GCN4* and the subsequent transcriptional induction of those genes required to alleviate the nutrient starvation.

We envisaged that 5MP1 overexpression might mimic the effect of eIF2 phosphorylation to confer 3AT resistance to the *gcn2Δ* strain. However, 5MP1 expression from the constitutive *SUI1* promoter or *GAL* promoter did not confer 3AT resistance to *gcn2Δ* strains (data not shown), although the abundance of 5MP1 expressed from *SUI1* and *GAL* promoters was ~12 (Figure 7B) and ~25-fold (see above) higher than that of yeIF2, respectively. We reasoned that eIF2B mutations known to limit TC levels could sensitize *gcn2Δ* strains to a reduction in eIF2 activities, which might be caused by 5MP1 expression. Indeed, alteration of either S576 or the AA-box 2 of the eIF2Bε catalytic domain (in the *gcd6-S576N gcn2Δ* and *gcd6-7A gcn2Δ* mutant strains, respectively) sensitizes the strains such that 5MP1 expression now increases the 3AT resistance (Figure 7A, Rows 3 and 8; Figure 7C, Row 3). It should be noted that these *gcd6* mutant strains are slightly resistant to high doses of 3AT (Figure 7A, Rows 2 and 7; Figure 7C, Row 2) (8,36) and that expression of 5MP1 provides further increase in this 3AT resistance. This growth of 5MP1-expressing strains suggests a modulatory role for 5MP1 in the regulation of translation initiation. However, its effect on yeast translation is only kinetic, as examined below, but may not be clearly physiological.

The overexpression of yeIF5 conferred much stronger growth in the presence of 3AT in the *gcn2Δ gcd6* strains than did 5MP1 (Figure 7A, Rows 5 and 10; Figure 7C, Row 5). This result may reflect either the fact that yeIF5 is expressed at a higher level than 5MP1 (Figure 7B), or that the yeIF5/yeIF2 interaction is stronger than 5MP1/yeIF2 interaction (Figure 2), or both. The enhanced resistance to histidine starvation shown by both excess eIF5 and 5MP1 was accompanied by corresponding increase in *HIS4-lacZ* expression, whose transcription is activated by Gcn4p (Figure 7D). Furthermore, both growth and *HIS4-lacZ* effects of 5MP1 are alleviated by the 5MP1 AA-box 2 mutation *7A* (Figure 7A, C and D) without decreasing 5MP1 abundance (Figure 7B). Overall, these results suggest that 5MP1 has the capacity to impact upon *GCN4* translation in a manner dependent upon its AA-box 2. Given the exquisite sensitivity of the *GCN4* system to changes in TC recruitment to the ribosome, these results further suggest that 5MP1 impacts upon the level or recruitment of TC to the pre-initiation complex.

5MP1 promotes eIF2 TC formation and inhibits MFC formation in yeast

A key question arising from the experiments described above is whether 5MP1 impacts upon the levels of

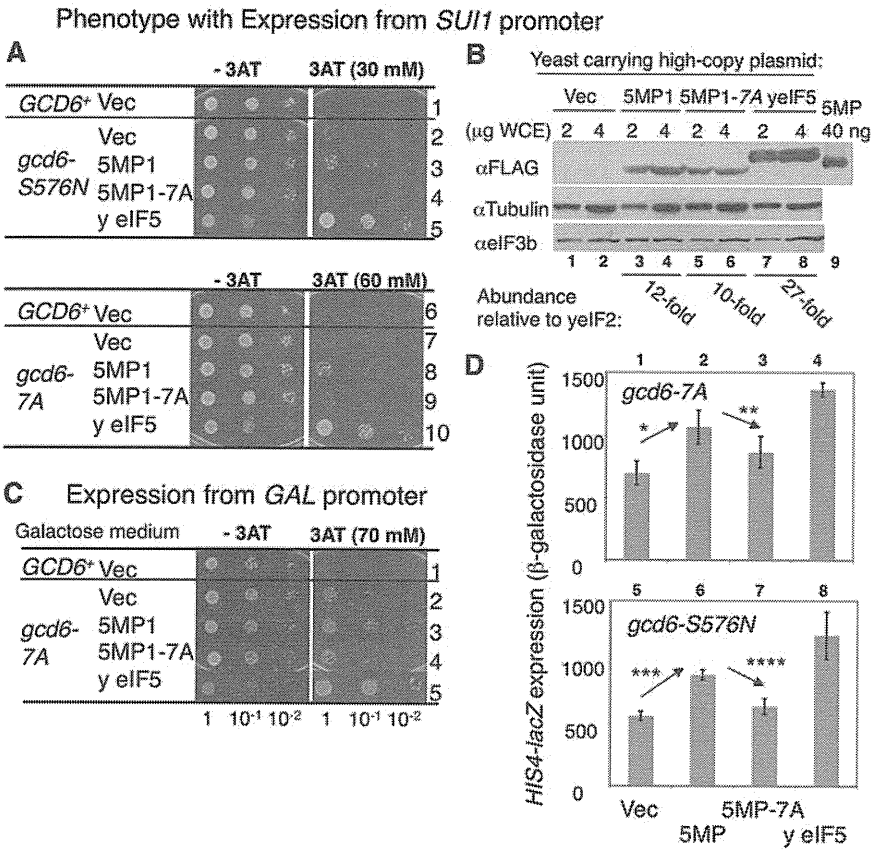

Figure 7. 5MP1 overexpression increases *GCN4* translation in *gcn2Δ gcd6* backgrounds. (**A**) Yeast dilution assays. Transformants of KAY16 (Row 1), GP3578 (Rows 2–5), KAY33 (Row 6) and KAY34 (Rows 7–10) carrying an empty vector (Vec), YEpL-FL-5MP1 (5MP1 in Row 3), YEpL-FL-5MP1-7A (5MP1-7A in Row 4), YEpTIF5-FL (yeIF5 in Row 5), YEpU-FL-5MP1 (5MP1 in Row 8), YEpU-FL-5MP1-7A (5MP1-7A in Row 9), and YEpU-TIF5 (yeIF5 in Row 10) were grown in SC-His-Leu or SC-His-Ura medium. Fixed amounts (A_{600} = 0.15) of the culture and its 10-fold serial dilutions were spotted onto the agar plates of the same medium without or with indicated amounts of 3AT and incubated at 30°C for 2 and 6 days, respectively. (**B**) Expression check. Indicated amounts of WCE prepared from KAY16 transformants carrying the plasmids used in (A) Rows 1–5 were subjected for immunoblotting with antibodies listed to the left. Bottom; molar amounts of FLAG-tagged proteins present in WCE were determined using 40 ng purified FL-5MP1 (lane 9) as standard, and compared to known amount of yeIF2 present in WCE (21). (**C**) Cultures of KAY33 (Row 1) or KAY34 (Rows 2–5) transformants carrying an empty vector (Vec), pEMBL-FL-5MP1 (5MP1), pEMGL-FL-5MP1-7A (5MP1-7A) and YEpU-TIF5 (yeIF5) were spotted and incubated as in (A), except that they were grown in SCGal-His-Ura medium. (**D**) Expression from chromosomally integrated *HIS4-lacZ* in transformants used in Panel A, Rows 10–13 and 5–8 were presented by β-galactosidase units. *P*-values for the differences indicated by arrows are: *, 0.004; **, 0.035; *** and ****, <0.00001.

complexes such as the TC or the multi-factor complex. To assess this, we quantified the abundance of yeIF2-containing complexes. For this purpose, the HA-tagged 5MP1 (HA-5MP1) was overexpressed in a strain encoding yeIF2β-FL (encoded by *SUI3-FL*), and the initiation components which co-immunoprecipitated with FLAG-eIF2 were quantitatively analyzed (21). Immunoblotting indicated that HA-5MP1 was expressed at approximately four to five times higher levels than yeIF5 (data not shown). As shown in Figure 8A, the expressed HA-5MP1 significantly increased TC levels ($P = 0.019$, $n = 7$), as determined by the amount of $tRNA_i^{Met}$ immunoprecipitated (see graph 1 to the right). The reason for this increase will be discussed below. Importantly, this TC increase was accompanied by a decrease in yeIF5 and yeIF3b that are co-associated with FL-yeIF2 (Figure 8A, graph 2 and 3, respectively, $P < 0.05$, $n = 3$). This decrease in the interaction of both eIF5 and eIF3 with FL-yeIF2 implicates HA-5MP1 in the inhibition of MFC formation.

To confirm and extend these observations, we next examined the impact of 5MP1 expression on the yeIF3-containing complexes. Hence, we overproduced FL-5MP1 in a strain encoding the HA-tagged yeIF3i subunit. As shown in Figure 8B, less yeIF2α co-precipitated with HA-yeIF3 in the presence of FL-5MP1 (lane 7) than in its absence (lane 6). Because eIF2/eIF3 association depends on bridging by eIF5, this is the hallmark of MFC formation. Thus, these results confirm that FL-5MP1 indeed inhibits MFC formation. The more dramatic effect on MFC relative to Figure 8A is likely due to a higher expression level of this FL-5MP1 construct than that of HA-5MP1. The 5MP1-mediated inhibition of MFC formation was alleviated by the AA-box 2 mutation *7A* introduced to FL-5MP1 (Figure 8B, lane 8). Since 5MP1 expression did not reduce the interaction of HA-yeIF3 with

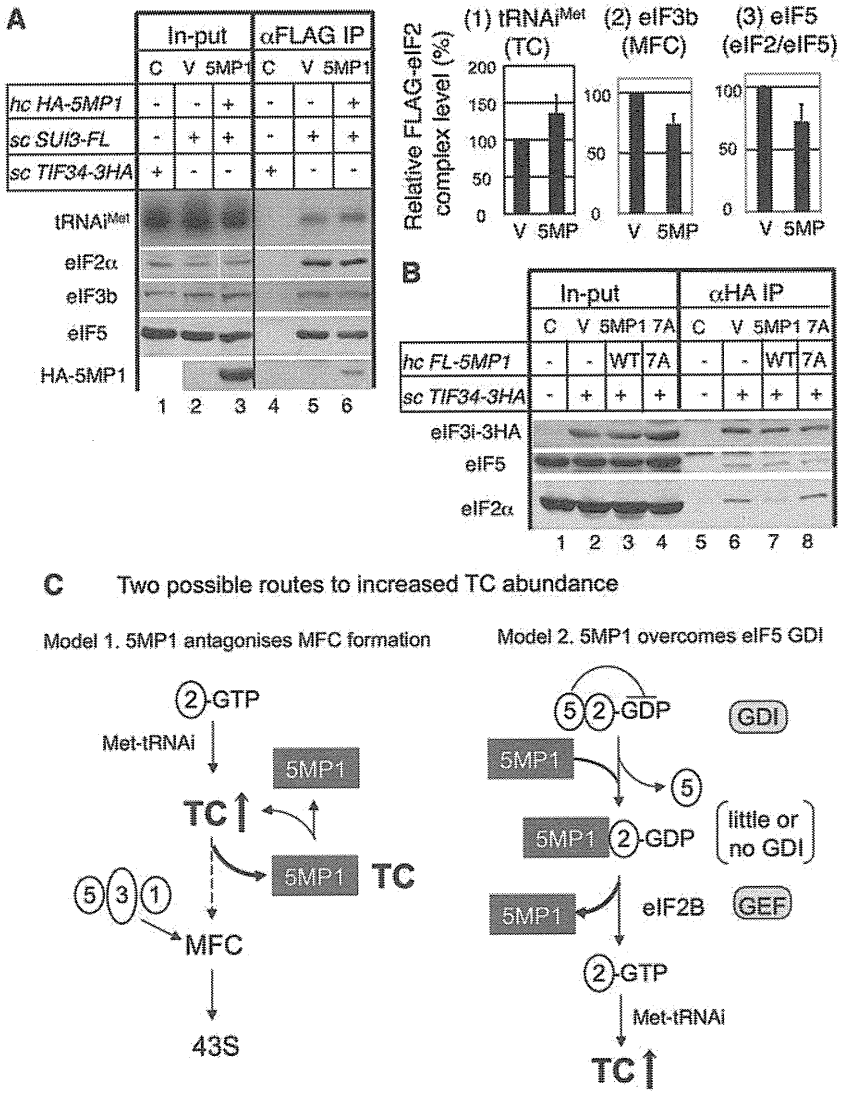

Figure 8. Effect of 5MP1 on the abundance of eIF complexes in yeast. (**A**) Quantitative anti-FLAG IP. An amount of 1 mg of WCE prepared from KAY107 (*TIF34-3HA*) transformant carrying an empty vector (C), KAY128 (*SUI3-FL*) transformants carrying an empty vector (V) or pEMBL-HA-5MP1 (5MP) was used for anti-FLAG IP and 80% (top gel) and 20% (bottom gels) of the precipitated fractions (lanes under αFLAG IP) were analyzed by northern and western blotting, respectively, with 2% in-put amount (lanes under In-put), as described (21). HA or FLAG-tagged alleles present in the transformants are indicated across the top. Graphs to the right summarize the relative amount of indicated components associated with FLAG-eIF2, after correction by the amount of eIF2α precipitated. (**B**) Co-IP with HA-eIF3. An amount of 200 μg of WCE prepared from KAY127 (*SUI3-FL*) transformant carrying an empty vector (C), KAY113 (*TIF34-3HA*) transformants carrying an empty vector (V), pEMBL-FL-5MP1 (HP), or pEMBL-FL-5MP-7A (7A) was used for anti-HA IP, and entire IP fractions and 10% in-put amounts were analyzed by immunoblotting with antibodies raised against HA-epitope (top) and yeast eIF2α (bottom). (**C**) Possible models to explain increased TC abundance by 5MP1 in yeast. Numbers in circles refer to eIFs (e.g. 1, eIF1). Gray squares, 5MP1. Model 1. 5MP1/TC interaction slows down MFC formation (dotted arrow). The accumulation of 5MP1/TC complex contributes to increase in overall TC abundance (both free TC and TC/5MP1). Model 2. 5MP1/eIF2-GDP interaction antagonizes the GDI function (stopped bar to GDP) of eIF5. The steps of GDI and GEF are highlighted with light gray round squares.

yeIF5 (Figure 8B), it seems that 5MP1 does not compete with yeIF3 binding to yeIF5 in yeast, consistent with the weak interaction observed between FL-5MP1 and yeIF3 (Figure 5D and E). These observations suggest that 5MP1 inhibits TC binding to the 40S subunit, primarily by sequestering TC away from yeIF5 and yeIF3, which otherwise promote TC binding to the 40S subunit (Figure 8C, Model 1). This would mean that an inhibition of TC recruitment would explain why 5MP1 enhanced *GCN4* translation in the *gcn2Δ gcd6* mutant strains (Figure 7).

DISCUSSION

In this article, we have assessed the function of the human MA3-W2 HEAT repeat protein previously called BZW2 and here renamed as 5MP1. We have shown that the

human 5MP1 directly interacts with eIF2 via the β subunit *in vitro* (Figure 2). Together with the finding that the 5MP1 *Drosophila* homolog, Kra, interacts with eIF2β, this result strengthens the idea that translation factors and regulators with the W2-type HEAT domains (i.e. eIF5, eIF2Bε and p97/NAT1/DAP5) can generally interact with eIF2. We also showed that 5MP can modulate overall translation (Figure 4C) and translation of a luciferase reporter gene in RRL (Figure 3A). These observations suggest that 5MP binding to eIF2 (and perhaps eIF3) can modulate the efficiency of protein synthesis.

How does 5MP regulate protein synthesis?

5MP interacts directly with eIF2 or eIF3 (Figure 2), and therefore could competitively inhibit or even replace the functional interactions of any of the W2-domain containing proteins such as eIF5 or eIF2Bε. Our *in vitro* studies directly examining the effect of 5MP on GDP binding to eIF2 showed that the human 5MP1 is not a GEF, but instead has weak GDI activity for eIF2 (Figure 5A). GDI activity was recently ascribed to yeast eIF5 as a second function in addition to its GAP activity (4). Therefore eIF5 GAP activity switches eIF2 into an inactive GDP-bound state, and its GDI activity prevents reactivation of eIF2 by the GEF eIF2B. Similarly the observed inhibition of GDP release by 5MP1 (GDI activity) could contribute to locking eIF2 in an inactive state; however, because 5MP1 GDI activity is weak, 5MP1/eIF2-GDP binding may antagonize eIF5 GDI and therefore promote GDP release. Consistent with this idea, we made an interesting observation that 5MP1 overexpression increases TC (eIF2-GTP-Met-tRNA$_i^{Met}$) abundance (Figure 8A). These observations led us to propose one mechanism for 5MP function (Figure 8C, Model 2). In this model, 5MP1 expression would compete directly with eIF5 GDI function, resulting in an increase in TC abundance by preventing eIF5 antagonizing the GEF activity of eIF2B. However an alternative explanation is also possible (see below).

The ability of 5MP1 to interact with both eIF2 and eIF3 (Figure 2A, B and D) strengthened the idea that 5MP1 could function as a competitive inhibitor and structural mimic of eIF5 functions in pre-initiation multifactor complex (MFC) assembly necessary for efficient translation initiation by the standard scanning model. This model is supported by a number of experimental observations. First, 5MP1 can bind eIF2β in competition with eIF5 (Figure 2C). Second, 5MP1 can compromise eIF5 co-migration with 40S ribosomes in the RRL (Figure 3B). Third, 5MP1 complex with yeast eIF2 does not include eIF5 (Figure 5D) and finally it can antagonize the binding of eIF2 TC to eIF3, which is necessary for MFC formation in yeast (Figure 8B). This latter observation provides an alternative explanation for the observed increase in TC levels following 5MP1 expression (Figure 8A). The observations are consistent with a fraction of TC becoming sequestered into a TC/5MP1 complex and being unavailable for MFC assembly. This idea is also shown diagrammatically in Figure 8C (Model 1). Thus, 5MP can act as a competitive inhibitor of eIF5 functions in promoting the assembly of the ribosomal pre-initiation complex, or act to antagonize eIF5 GDI function and thereby act positively to promote GEF function. Either or both of the models together could account for the observed increase in TC. We also acknowledge that the effect of the human 5MP1 on yeast translation is overall weak and not clearly physiological, perhaps owing to the evolutionary distance from the model organism. To take better advantage of the yeast system, it would be attractive to study the effect of 5MP from lower eukaryotes (16), those from fungi (Basidiomycota), in particular.

Is 5MP a part of inhibitory mRNP complexes?

The models proposed in Figure 8C consider the inhibitory effect of 5MP1 on eIF2, as observed in yeast. Because 5MP1 can also interact with eIF3 (Figure 2D), its effect on translation in mammalian cells could be more complex. For example, with a link to eIF3, 5MP1 that lacks the GAP domain might replace eIF5 recruitment to the 40S subunit (Figure 3B) and thereby prevent 60S subunit joining. An alternative, but not mutually exclusive, idea consistent with its partial effect on translation in mammalian cells (Figure 4C) is that effective translational control by this protein requires additional binding proteins in complex with 5MP1, eIF2 and eIF3. In agreement with this idea, evidence was provided previously that the *Drosophila* homolog Kra binds simultaneously to eIF2 and Shot, a cytoskeletal element. Furthermore, Kra co-expresses with the mRNA-specific binding factors Pumilio and Staufen in certain areas of the central nervous system, suggesting that Kra is a component of multiple inhibitory mRNA/protein (mRNP) complexes (20). Specific expression of Kra in cholinergic local neurons of antennal lobe has been established and a *krasavietz* enhancer trap line is frequently used to study *Drosophila* CNS function (37). Together these findings suggest an intriguing possibility that 5MP1 and eIF2 form part of a larger translationally repressed mRNA complex that are undergoing cytoskeleton-mediated intracellular transport. The observed GDI activity of 5MP1 (Figure 5A), if it occurs *in vivo*, would inhibit GDP dissociation during the transport process in favor of translational inhibition. A 5MP interaction with cytoskeletal elements in humans was suggested previously by the physical interaction of human BZW1/5MP2 with PSTPIP1 (38), which in turn interacts with Wiskott-Aldrich Syndrome Protein (39). The latter two proteins, which regulate F-actin formation, are expressed predominantly in hematopoietic cells, where higher levels of BZW1/5MP2 transcripts are also observed (40). Although work to address these ideas is beyond the scope of the present manuscript, it is one avenue to pursue in the future.

SUPPLEMENTARY DATA

Supplementary Data are available at NAR Online.

ACKNOWLEDGEMENTS

Special thanks are due to John Hershey and Masaaki Sokabe for purified human eIF2 and eIF3 and Hans Gross for critical reading of the manuscript. The authors also thank Assen Marinchev and Gota Kawai for advice on 5MP structure, Futoshi Shibasaki for anti-eIF3e, Alan Hinnebusch, Tom Donahue, John McCarthy and Tom Dever for antibodies against yeast eIFs, Miwako Homma for human eIF5 plasmids and members of Ashe and Pavitt labs for frank discussion.

FUNDING

National Institutes of Health GM64781, NCRR K-INBRE Pilot Grant P20 RR016475; K-state Terry Johnson Cancer Center (to K.A.); NIDCR intramural grant (to J.A.C.); GM49164 (to R.C.W.); BBSRC grants BB/E002005/1 and BB/H010599/1 (to G.D.P.); and short-term fellowship for his sabbatical to Manchester, UK in Feb-Mar, 2008 (to K.A.). Funding for open access charge: K-state Terry Johnson Cancer Center.

Conflict of interest statement. None declared.

REFERENCES

1. Pestova,T.V., Lorsch,J.R. and Hellen,C.U.T. (2007) The mechanism of translation initiation in eukaryotes. In Mathews,M.B., Sonenberg,N. and Hershey,J.W.B. (eds), *Translational Control in Biology and Medicine*. Cold Spring Harbor Lab Press, Cold Spring Harbor, NY, pp. 87–128.
2. Hinnebusch,A.G., Dever,T.E. and Asano,K. (2007) Mechanism of translation initiation in the yeast *Saccharomyces cerevisiae*. In Mathews,M.B., Sonenberg,N. and Hershey,J.W.B. (eds), *Translational Control in Biology and Medicine*. Cold Spring Harbor Lab Press, Cold Spring Harbor, NY, pp. 225–268.
3. Singh,C.R., Lee,B., Udagawa,T., Mohammad-Qureshi,S.S., Yamamoto,Y., Pavitt,G.D. and Asano,K. (2006) An eIF5/eIF2 complex antagonizes guanine nucleotide exchange by eIF2B during translation initiation. *EMBO J.*, **25**, 4537–4546.
4. Jennings,M.D. and Pavitt,G.D. (2010) eIF5 has GDI activity necessary for translational control by eIF2 phosphorylation. *Nature*, **465**, 378–381.
5. Andrade,M.A., Petosa,C., O'Donoghue,S.I., Muller,C.W. and Bork,P. (2001) Comparison of ARM and HEAT protein repeats. *J. Mol. Biol.*, **309**, 1–18.
6. Marintchev,A., Edmonds,K.A., Maritcheva,B., Hendrickson,E., Oberer,M., Suzuki,C., Herby,B., Sonenberg,N. and Wagner,G. (2009) Topology and regulation of the human eIF4A/4G/4H helicase complex in translation initiation. *Cell*, **136**, 447–460.
7. Raught,B. and Gigras,A.-C. (2007) Signaling to Translation Initiation. In Mathews,M.B., Sonenberg,N. and and Hershey,J.W.B. (eds), *Translational Control in Biology and Medicine*. Cold Spring Harbor Lab Press, Cold Spring Harbor, NY, pp. 369–400.
8. Asano,K., Krishnamoorthy,T., Phan,L., Pavitt,G.D. and Hinnebusch,A.G. (1999) Conserved bipartite motifs in yeast eIF5 and eIF2Bε, GTPase-activating and GDP-GTP exchange factors in translation initiation, mediate binding to their common substrate eIF2. *EMBO J.*, **18**, 1673–1688.
9. Yamamoto,Y., Singh,C.R., Marintchev,A., Hall,N.S., Hannig,E.M., Wagner,G. and Asano,K. (2005) The eukaryotic initiation factor (eIF) 5 HEAT domain mediates multifactor assembly and scanning with distinct interfaces to eIF1, eIF2, eIF3 and eIF4G. *Proc. Natl Acad. Sci. USA*, **102**, 16164–16169.
10. Gomez,E., Mohammad,S.S. and Pavitt,G.P. (2002) Characterization of the minimal catalytic domain within eIF2B: the guanine-nucleotide exchange factor for translation initiation. *EMBO J.*, **21**, 5292–5301.
11. Asano,K., Clayton,J., Shalev,A. and Hinnebusch,A.G. (2000) A multifactor complex of eukaryotic initiation factors eIF1, eIF2, eIF3, eIF5, and initiator $tRNA^{Met}$ is an important translation initiation intermediate in vivo. *Genes Dev.*, **14**, 2534–2546.
12. Imataka,H., Olsen,S. and Sonenberg,N. (1997) A new translational regulator with homology to eukaryotic translation initiation factor 4G. *EMBO J.*, **16**, 817–825.
13. Yamanaka,S., Zhang,X.Y., Maeda,M., Miura,K., Wang,S., Farese,R.V. Jr, Iwao,H. and Innerarity,T.L. (2000) Essential role of NAT1/p97/DAP5 in embryonic differentiation and the retinoic acid pathway. *EMBO J.*, **19**, 5533–5541.
14. Lee,S.H. and McCormick,F. (2006) p97/DAP5 is a ribosome-associated factor that facilitates protein synthesis and cell proliferation by modulating the synthesis of cell cylce proteins. *EMBO J.*, **25**, 4008–4019.
15. Liberman,N., Dym,O., Unger,T., Albeck,S., Peleg,Y., Jacobovitch,Y., Branzburg,A., Eisenstein,M., Marash,L. and Kimchi,A. (2008) The crystal structure of the C-terminal DAP5/p97 domain sheds light on the molecular basis for its processing by caspase cleavage. *J. Mol. Biol.*, **383**, 539–548.
16. Marintchev,A. and Wagner,G. (2005) eIF4G and CBP80 share a common origin and similar domain organization: Implications for the structure and function of eIF4G. *Biochemistry*, **44**, 12265–12272.
17. Mitra,P., Vaughan,P.S., Stein,J.L., Stein,G.S. and van Wijnen,A.J. (2001) Purification and functional analysis of a novel leucine-zipper/nucleotide-fold protein, BZAP45, stimulating cell cycle regulated histone H4 gene transcription. *Biochemistry*, **40**, 10693–10699.
18. Hoya,M.R., Wahlestedt,C. and Höög,C. (2000) A visual intracellular classification strategy for uncharacterized human proteins. *Exp. Cell Res.*, **259**, 239–246.
19. Lee,S., Nahm,M., Lee,M., Kwon,M., Kim,E., Zadeh,A.D., Cao,H., Kim,H.-J., Lee,Z.E., Oh,S.B. *et al.* (2007) The F-actin-microtubule crosslinker Shot is a platform for Krasavietz-mediated translational regulation of midline axon repulsion. *Development*, **134**, 1767–1777.
20. Dubnau,J., Chiang,A.-S., Grady,L., Barditch,J., Gossveiler,S., McNeil,J., Smith,P., Buldoc,F., Scott,R., Certa,U. *et al.* (2003) The staufen/pumilio pathway is involved in Drosophila long-term memory. *Curr. Biol.*, **13**, 286–296.
21. Singh,C.R., Udagawa,T., Lee,B., Wassink,S., He,H., Yamamoto,Y., Anderson,J.T., Pavitt,G.D. and Asano,K. (2007) Change in nutritional status modulates the abundance of critical pre-initiation intermediate complexes during translation initiation in vivo. *J. Mol. Biol.*, **370**, 315–330.
22. Mohammad-Qureshi,S.S., Haddad,R., Palmer,K.S., Richardson,J.P. and Pavitt,G.D. (2007) Purification of FLAG-tagged eukaryotic initiation factor 2B complexes, subcomplexes, and fragments from Saccharomyces cerevisiae. *Methods Enzymol.*, **431**, 1–13.
23. Homma,M.K., Wada,I., Suzuki,T., Yamaki,J., Krebs,E.G. and Homma,Y. (2005) CK2 phosphorylation of eukaryotic translation initiation factor 5 potentiates cell cylce progression. *Proc. Natl Acad. Sci. USA*, **102**, 15688–15693.
24. Singh,C.R. and Asano,K. (2007) Localization and characterization of protein-protein interaction sites. *Methods Enzymol.*, **429**, 139–161.
25. Asano,K., Lon,P., Krishnamoorthy,T., Pavitt,G.D., Gomez,E., Hannig,E.M., Nika,J., Donahue,T.F., Huang,H.-K. and Hinnebusch,A.G. (2002) Analysis and reconstitution of translation initiation in vitro. *Methods Enzymol.*, **351**, 221–247.
26. Teske,B.F., Baird,T.D. and Wek,R.C. (2011) Methods for analyzing eIF2 kinases and translational control in the unfolded protein response. *Methods Enzymol.*, **493**, 333–356.
27. Das,S. and Maitra,U. (2000) Mutational analysis of mammalian translation initiation factor 5 (eIF5): role of interaction between the beta subunit of eIF2 and eIF5 in eIF5 function in vitro and in vivo. *Mol. Cell. Biol.*, **20**, 3942–3950.
28. Vattem,K.M. and Wek,R.C. (2004) Reinitiation involving upstream ORFs regulates ATF4 mRNA translation in mammalian cells. *Proc. Natl Acad. Sci. USA*, **101**, 11269–11274.

29. Fukao,A., Sasano,Y., Imataka,H., Inoue,K., Sakamoto,H., Sonenberg,N., Thoma,C. and Fujiwara,T. (2009) The ELAV protein HuD stimulates cap-dependent translation in a poly(A)- and eIF4A-dependent manner. *Mol. Cell*, **36**, 1007–1017.
30. Conte,M.R., Kelly,G., Babon,J., Sanfelice,D., youell,J., Smerdon,S.J. and Proud,C.G. (2006) Structure of the eukaryotic initiation factor 5 reveals a fold common to several translation factors. *Biochemistry*, **45**, 4550–4558.
31. Hoyle,N.P., Castelli,L.M., Campbell,S.G., Holmes,L.E. and Ashe,M.P. (2007) Stress-dependent relocalization of translationally primed mRNPs to cytoplasmic granules that are kinetically and spatially distinct from P-bodies. *J. Cell Biol.*, **179**, 65–74.
32. Buchan,J.R., Muhlrad,D. and Parker,R. (2008) P bodies promote stress granule assembly in Saccharomyces cerevisiae. *J. Cell Biol.*, **183**, 441–455.
33. Grousl,T., Ivanov,P., Frýdlová,I., Vasicová,P., Janda,F., Vojtová,J., Malínská,K., Malcová,I., Nováková,L., Janosková,D. *et al.* (2009) Robust heat shock induces eIF2alpha-phosphorylation-independent assembly of stress granules containing eIF3 and 40S ribosomal subunits in budding yeast, Saccharomyces cerevisiae. *J. Cell Sci.*, **122**, 2078–2088.
34. Campbell,S.G., Hoyle,N.P. and Ashe,M.P. (2005) Dynamic cycling of eIF2 through a large eIF2B-containing cytoplasmic body: implications for translational control. *J. Cell Biol.*, **170**, 925–934.
35. Hinnebusch,A.G. (2005) Translational regulation of gcn4 and the general amino acid control of yeast. *Annu. Rev. Microbiol.*, **59**, 407–450.
36. Gomez,E. and Pavitt,G.D. (2000) Identification of domains and residues within the epsilon subunit of eukaryotic translation initiation factor 2B (eIF2β) required for guanine nucleotide exchange reveals a novel activation function promoted by eIF2B complex formation. *Mol. Cell Biol.*, **20**, 3965–3976.
37. Shang,Y., Claridge-Chang,A., Sjulson,L., Pypaert,M. and Miesenbock,G.M. (2007) Excitatory local circuits and their implications for alfactory processing in the fly antennal lobe. *Cell*, **128**, 601–612.
38. Ewing,R.M., Chu,P., Elisma,F., Li,H., Taylor,P., Climie,S., McBroom-Cerajewski,L., Robinson,M.D., O'Connor,L., Li,M. *et al.* (2007) Large-scale mapping of human protein-protein interactions by mass spectrometry. *Mol. Syst. Biol.*, **3**, 89.
39. Wu,Y., Spencer,S.D. and Lasky,L.A. (1999) Trysine phosphorylation regulates the SH3-mediated binding of the Wiskott-Aldrich Syndome protein to PSTPIP, a cytoskeletal-associated protein. *J. Biol. Chem.*, **273**, 5765–5770.
40. Chunlei,W., Orozco,C., Boyer,J., Leglise,M., Goodale,J., Batalov,S., Hodge,C.L., Haase,J., Janes,J., Huss,J.W. *et al.* (2009) BioGPS: an extensible and customizable portal for querying and organizing gene annotation resources. *Genome Biol.*, **10**, R130.
41. Chen,L., Uchida,K., Endler,A. and Shibasaki,F. (2007) Mammalian tumor suppressor Int6 specifically targets hypoxia inducible factor 2alpha for degradation by hopoxia- and pVHL-independent regulation. *J. Biol. Chem.*, **282**, 12707–12716.

mTOR Signaling, Function, Novel Inhibitors, and Therapeutic Targets

Ryosuke Watanabe, Liu Wei, and Jing Huang

Department of Molecular and Medical Pharmacology, David Geffen School of Medicine, Jonsson Comprehensive Cancer Center, and the Molecular Biology Institute, University of California, Los Angeles, California

Mammalian target of rapamycin (mTOR) is an evolutionally conserved serine/threonine kinase that integrates signals from multiple pathways, including nutrients (e.g., amino acids and glucose), growth factors (e.g., insulin and insulinlike growth factor 1), hormones (e.g., leptin), and stresses (e.g., starvation, hypoxia, and DNA damage) to regulate a wide variety of eukaryotic cellular functions, such as translation, transcription, protein turnover, cell growth, differentiation, cell survival, metabolism, energy balance, and stress response. Dysregulation of the mTOR pathway is closely associated with cancers and other human diseases. Thus, mTOR is of considerable interest in view of its potential as a therapeutic drug target. However, only limited success has been achieved in clinical applications of mTOR inhibitors because of the inherent complexity in the regulation and function of mTOR. Emerging new developments in this area, such as novel readouts (potential biomarkers) for mTOR activity, dynamic assembly and translocation of the mTOR complex, cross-regulation between mTOR complex 1 and mTOR complex 2 via inter- and intracomplex loops, new mTOR regulators, and new inhibitors, are providing insights that may help overcome these challenges. The introduction of innovative imaging strategies is also expected to give rise to breakthroughs in understanding mTOR network complexity and mTOR inhibitor action by visualizing the regulation and function of mTOR.

Key Words: mTOR structure; mTOR therapy; mTORC

J Nucl Med 2011; 52:497–500
DOI: 10.2967/jnumed.111.089623

Mammalian target of rapamycin (mTOR) is one of the protein kinases related to phosphatidylinositol 3-kinase and structurally contains an N-terminal HEAT repeat domain and a C-terminal kinase domain flanked by FAT and FATC domains (Fig. 1). mTOR exists in 2 functionally and structurally distinct complexes, rapamycin-sensitive mTOR complex 1 (mTORC1) and rapamycin-insensitive mTOR complex 2 (mTORC2), which becomes rapamycin-sensitive after prolonged rapamycin treatment (Fig. 2). mTORC1 phosphorylates S6K and 4E-BP1 (which are used as a readout for mTORC1 activity) and regulates translation, autophagy, growth, lipid biosynthesis, mitochondria biogenesis, and ribosome biogenesis, whereas mTORC2 phosphorylates SGK1, Akt (S473 phosphorylation is used as a readout for mTORC2 activity), Rac1, and PKCα and regulates survival, metabolism, proliferation, and cytoskeletal organization (*1,2*).

mTOR interacts with Tel2 (also known as TELO2 and hCLK2) and FXBW7 (Fig. 1). Deletion of Tel2 results in destabilization of mTOR, whereas FBXW7 targets mTOR for ubiquitin-proteasome–dependent degradation (*3,4*). mTOR also interacts with Raptor, which is a specific component of mTORC1, through binding to the N-terminal HEAT domain (Figs. 1 and 2). Raptor functions as a scaffold protein to recruit S6K and 4E-BP1 to promote protein synthesis through the direct phosphorylation of S6K and 4E-BP1 by mTORC1 (Fig. 2) (*5*). Overexpression of Rictor, a specific component of mTORC2, disrupts mTOR–Raptor interaction. This indicates that Rictor may compete with Raptor in binding to mTOR through the HEAT domain. DEPTOR, an inhibitory protein for mTOR, binds through the FAT domain of mTOR, and overexpression of DEPTOR results in the suppression of S6K by inhibiting Akt, whereas loss of DEPTOR activates S6K and Akt.

Rapamycin, the best-characterized mTOR inhibitor, binds to FKBP12, which in turn targets mTOR through its FRB domain, resulting in an inhibition of mTOR function. Mutation of a conserved serine (aa 2035 in human mTOR) in the FRB domain confers resistance to rapamycin (*6*). Amino acid regulates dynamic assembly and translocation of mTORC1 with FKBP38 and Rag guanosine triphosphatase (GTPase) (*5*). Mitochondrial membrane protein FKBP38 is an endogenous inhibitor of mTOR and binds to the FRB domain of mTOR (*7*). mTOR–FKBP38 interaction is increased by amino acid or serum starvation, leading to inhibition of mTOR activity. The Rheb GTPase protein also binds to the FRB domain of mTOR and is involved in mTOR activation by amino acids. On amino acid stimulation, 4 members of the Rag subfamily of Ras small GTPases—RagA, RagB, RagC, and RagD—bind to Raptor directly, and Rag-bound mTORC1 translocates to Rab7 (a GTPase required for transporter degradation)-positive perinuclear vesicular structures, where Rheb localizes. This relocalization enables mTORC1 binding to Rheb, leading to mTORC1 kinase activation. Ragulator recruits Rag family proteins and mTORC1 to lysosomes to activate mTORC1 (*8*). mLST8 binds to the kinase domain of mTOR and strongly enhances mTOR signaling. Knockout studies demonstrated that mSLT8 is required to maintain the Rictor-mTOR, but not the Raptor-mTOR,

Received Jul. 1, 2010; revision accepted Feb. 23, 2011.
For correspondence or reprints contact: Ryosuke Watanabe, Department of Molecular and Medical Pharmacology, UCLA, Box 951735, 23-231A CHS, Los Angeles, CA 90095-1735.
E-mail: ryosukewatanabe@mednet.ucla.edu

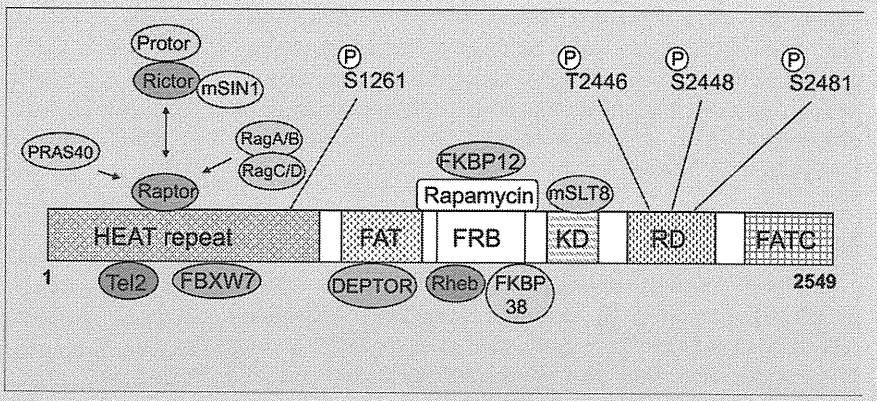

FIGURE 1. mTOR, its interacting proteins, and phosphorylation sites. DEPTOR = DEP domains and its specific interaction with mTOR; FAT = FRAP, ATM, TRRAP; FATC = FRAP ATM TRRAP carboxy terminus; FKBP = FK506 binding protein; FKBP12 = 12-kDa immunophilin FK506-binding protein; FRB = FKBP12 rapamycin-binding; FXBW7 = F-box and WD repeat domain–containing 7 (also known as hCDC4, FBW7, and hAGO); HEAT = Huntington, elongation factor 3, PR65/A, TOR; KD = kinase domain; mSLT8 = mammalian homolog of lethal with sec-13 gene 8; PRAS40 = proline-rich Akt substrate, 40 kDa; Protor = protein observed with Rictor-1; Rag = ras-related GTP-binding protein; Raptor = regulatory associated protein of mTOR; RD = regulatory domain; Rheb = Ras homolog enriched in brain; Rictor = rapamycin-insensitive companion of mTOR. Four mTOR phosphorylation (P) sites (S1261, T2446, S2448, and S2481) and mTOR-interacting proteins are indicated.

interaction regardless of the fact that both mTORC1 and mTORC2 contain mSLT8, indicating the mTORC2-specific role of mSLT8 (*9*).

PHOSPHORYLATION OF MTOR

There are 4 characterized phosphorylation sites in mTOR (Fig. 1). T2446 is regulated by nutrient availability and is probably phosphorylated by adenosine monophosphate kinase (AMPK). S2448 is phosphorylated by S6K, which directly reflects amino acid and nutrient status. S2481 was known as a rapamycin-insensitive autophosphorylation site. mTORC1 contains mainly mTOR phosphorylated at S2448, whereas mTORC2 contains predominantly mTOR phosphorylated at S2481, sensitive to short versus prolonged rapamycin treatment, respectively (*10*). The finding that mTORC1 also contains mTOR phosphorylated on S2481 in the same cell line and that the phosphorylation on S2481 in both mTORC1 and mTORC2 is sensitive to wortmannin, a phosphatidylinositol 3–kinase inhibitor (*11*), indicates that insulin signals via phosphatidylinositol 3–kinase to promote mTORC1 and mTORC2-associated mTOR autophosphorylation on S2481. These discrepancies between previous and more recent work are likely due to the fact that existence of mTORC1 and mTORC2 with different sensitivities to rapamycin was apparent only later. S1261

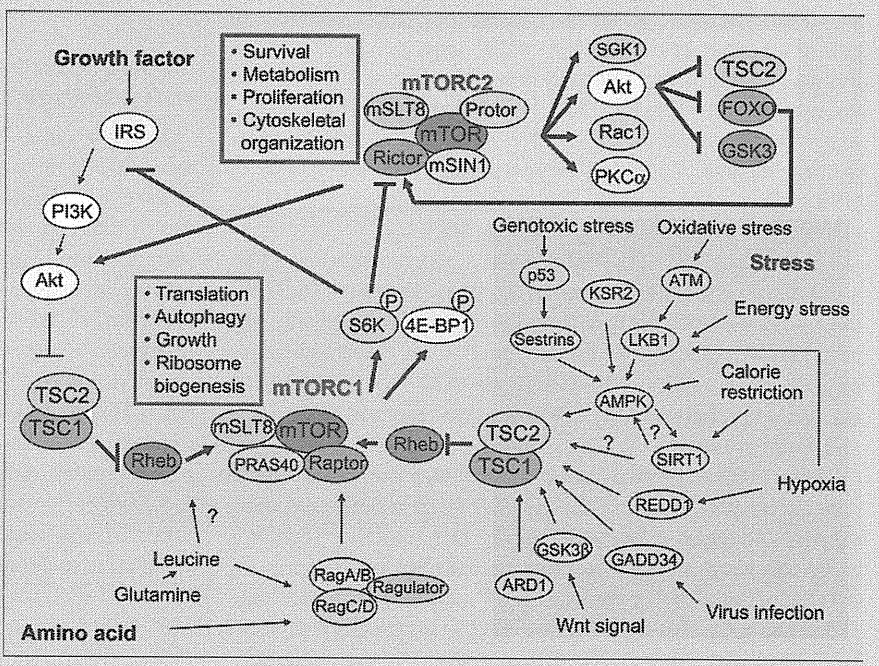

FIGURE 2. mTOR complexes and mTOR signaling network. ARD1 = arrest-defective protein 1; ATM = ataxia telangiectasia, mutated; 4E-BP1 = eukaryotic initiation factor 4E-binding protein 1; FOXO = forkhead box O; GADD34 = growth arrest and DNA damage; GSK3 = glycogen-synthase-kinase-3; IRS = insulin receptor substrate; KSR2 = kinase suppressor of Ras 2. PI3K = phosphoinositide-3-kinase; PKC = protein kinase C; Rac1 = ras-related C3 botulinum toxin substrate 1; REDD1 = regulated in development and DNA damage response genes 1; SGK1 = glucocorticoid inducible kinase-1; S6K = ribosomal protein S6 kinase; TSC1/2 = tuberous sclerosis 1/2. Selected components and functions of both mTOR1 and mTORC2 are indicated, and both mTORC1 and mTORC2 additionally interact with DEPTOR, which usually inhibits the activity of both complexes. Growth factor such as insulin stimulates mTORC1 (and probably also mTORC2), leading to Akt activation to inhibit TSC2, a GTPase activating protein for Rheb. Amino acid also activates mTORC1 through glutamine-leucine and Rag–Ragulator complex, which is required for full activation of mTORC1 by growth factor. Little is known about activation mechanism of mTORC2. Feedback loop by S6K-IRS or S6K-Rictor exists in mTOR signaling. In contrast, cellular stress activates TSC2 and inhibits mTOR pathway.

within the HEAT domain is phosphorylated by insulin/phosphatidylinositol 3–kinase in an amino acid–dependent, rapamycin-insensitive, and autophosphorylation-independent manner. S1261 phosphorylation promotes the phosphorylation of S6K and 4E-BP1, and mutation on S1261 attenuates phosphorylation on S2481.

FEEDBACK LOOPS

Feedback loops are an important mechanism to regulate mTOR signaling (Fig. 2). mTORC1-stimulated S6K inhibits IRS through multiple phosphorylation sites on IRS, resulting in its degradation. S6K also phosphorylates Rictor at T1135 (*12*). Mutation at T1135 on Rictor results in increased phosphorylation of Akt at S473 and its downstream target, FOXO1/3a and GSK3α/β. Knockdown of Rictor results in an unchanged or a slight increase in the phosphorylation of S6K, indicating that mTORC1 and mTORC2 cross-regulate their activities through S6K and Rictor. Stress-activated FOXO increases the amount of Rictor and upregulates mTORC2 activity but downregulates mTORC1 activity (*13*). In this regard, identification and characterization of mTORC1 and mTORC2 were an important step toward understanding and visualizing the behavior of the mTOR complex structurally and functionally.

INHIBITORY MECHANISMS OF MTOR SIGNALING PATHWAY

Under low energy (high adenosine monophosphate–to–adenosine triphosphate ratio), AMPK is activated in an LKB1-dependent manner to phosphorylate TSC2 (Fig. 2) (*2*). AMPK also directly phosphorylates Raptor at S792 in an LKB1-dependent manner, which is required for the inhibition of mTORC1 and growth arrest under energy stress. Under hypoxic conditions, hypoxia-inducible factor 1–mediated upregulation of REDD1 and REDD2 proteins by hypoxia leads to the activation of TSC1/2 in an LKB1-AMPK–independent manner. TSC2 has been reported to be a substrate of GSK3, and activation of the Wnt pathway stimulates the mTOR pathway by phosphorylating TSC2 by GSK3.

Under high levels of cellular reactive oxygen species, ATM, a regulator of the DNA damage response, activates TSC2 via the LKB1-AMPK pathway to inhibit the mTOR pathway and to induce autophagy (*14*). Rapamycin inhibits elevated reactive oxygen species and mTOR activity in ATM−/− cells, indicating cross-talk between the DNA damage response and energy metabolic pathway.

GADD34 is induced by almost all cellular stresses and binds and dephosphorylates TSC2. GADD34−/− cells are more sensitive to glucose starvation and virus infection than WT cells, resulting in apoptosis due to inability to suppress the mTOR pathway (*15*). Treatment of rapamycin indeed suppresses apoptosis in GADD34−/− cells, suggesting that stress stimuli inhibit the mTOR pathway through the GADD34-TSC2 axis.

Recently, an acetylation-mediated TSC2 regulation was reported (*16*). ARD1, an acetyltransferase and a putative tumor suppressor, binds, acetylates, and stabilizes TSC2, leading to inhibition of the mTOR pathway. The expression of ARD1 correlates with that of TSC2 in multiple tumor types, and loss of heterozygosity at the ARD1 locus was observed in human breast, lung, pancreatic, and ovarian cancer samples.

KSR2, a regulator of extracellular signal-regulated kinase 1/2 (a mitogen-activated protein kinase), binds and modulates the activity of AMPK. KSR2 regulates AMPK-dependent glucose uptake and fatty acid oxidation, and KSR2 knockout mice show decreased fatty acid oxidation and thermogenesis resulting in obesity (*17*).

Three sestrin family proteins inhibit the mTOR pathway through the AMPK-TSC2 axis. p53 target genes Sestrin1 and Sestrin2 are induced on oxidative stress and DNA damage and bind and activate AMPK, resulting in TSC2-dependent inhibition of the mTOR pathway (*18*). The expression of mammalian Sestrin3 is regulated by Akt in a FOXO3a-dependent manner and activates AMPK and regulates cellular reactive oxygen species accumulation (*13,19*). Increased reactive oxygen species caused by accelerated oxygen consumption in Akt1/2 knockout cells was reduced by knockdown of Sestrin3, indicating that Sesn3 plays an important role in the regulation of cellular reactive oxygen species mediated by Akt and FOXO (*19*).

Sirtuin 1 (SIRT1) is a nicotinamide adenine dinucleotide (NAD^+)–dependent deacetylase that has been implicated in regulation of the mTOR pathway. Although SIRT1 deacetylates LKB1 for the LKB1-AMPK activation, AMPK may regulate SIRT1 activity by increasing intracellular NAD^+. AMPK kinase activity is required to trigger SIRT1-dependent response to exercise and fasting, but it remains unknown whether AMPK is required for fasting-induced activation of SIRT1 and deacetylation of its targets (*20*). Further studies will be required to determine the interdependence of AMPK and SIRT1 on the mTOR pathway.

MTOR INHIBITORS IN CLINICAL TRIALS AND THE NEED FOR COMPANION BIOMARKERS

Because more than 80% of human cancers acquire hyperactivation of the mTOR pathway, rapamycin has been expected to have powerful anticancer effects. The effects of the combined use of rapalogs with other anticancer agents or rapalogs alone are under investigation in several human cancers, such as brain, breast, and other solid tumors (*21,22*). More complex than expected, so far rapalogs have achieved only limited success in cancer treatment, perhaps because of cell type–dependent sensitivity to rapamycin, feedback loops, rapamycin-independent mTOR function (e.g., phosphorylation of 4E-BP1), development of resistance to rapamycin, inadequate drug delivery to tumor targets, and insufficient understanding of the molecular mechanism by which rapamycin inhibits mTOR and cell growth (even today, exactly how rapamycin perturbs mTOR function is not completely understood). Dual mTOR–phosphatidylinositol 3–kinase inhibitors, such as NVP-BEZ235 and PI-103, and a different class of mTOR inhibitors (e.g., Torin1, PP242, PP30, Ku-0063794, WAY-600, WYE-687, WYE-354, and CC-223) that act through the canonic kinase inhibitor mechanism by targeting the adenosine triphosphate–binding pocket of the mTOR kinase domain, have been developed, and their anticancer effects are being investigated (*23*).

When one is considering effective therapy with rapalogs and other anticancer agents, the concept of synthetic lethality may help overcome many of the problems described above (*24,25*). We envision that these agents may be used in combination therapy with rapamycin to yield the following benefits: to sensitize a tumor's response to rapamycin, to provide a synthetic lethal strategy against rapamycin-insensitive tumors, and to prevent or delay the development of rapamycin resistance in tumors (analogous to the successful use of drug cocktails for treating HIV infection).

Several biomarkers have been developed to monitor the effects of mTOR inhibitors. These include measurements by Western blot or immunohistochemistry of S6K and 4E-BP1 phosphorylation and of various immunocytokines, including interleukin 2, 4, and 10. Because these methods may lack the required selectivity and sensitivity, there is a clear need for the identification and validation of new biomarker sets to predict and monitor responses to mTOR inhibitors. The combined use of different classes of biomarkers may be needed to accurately predict responses to mTOR inhibitors (*26*). In particular, similar to the revolutionary use of ^{18}F-FDG (a glucose analog) (*27*), and 3′-deoxy-3′-^{18}F-fluorothymidine (^{18}F-FLT) (a thymidine analog) (*28*), discovery of endogenous small-molecule surrogate biomarkers should enable the development of real-time noninvasive molecular imaging agents that will find immediate utility in the clinic both for drug therapy monitoring and for new drug development and trials. PET with ^{18}F-FDG and ^{18}F-FLT for monitoring tumor responses to mTOR inhibitors has been evaluated in preclinical and clinical studies. It has been shown in mice that rapamycin significantly reduced the ^{18}F-FDG and ^{18}F-FLT uptake in human U87 glioma xenografts (*29*). In another study, the mTOR inhibitor everolimus (RAD001) induced a strong inhibition of ^{18}F-FLT uptake in human SKOV3 ovarian cancer xenografts (*30*). Recently, promising results were observed in a phase I clinical trial with the mTOR inhibitor RAD001 in glioma patients. In this study, ^{18}F-FDG PET revealed partial metabolic responses in a subset of patients. Collectively, these preliminary results are encouraging, and they should provide the impetus for more extensive studies to validate such PET biomarkers for monitoring therapeutic interventions using mTOR inhibitors.

ACKNOWLEDGMENTS

We thank Caius Radu for critical reading and comments on the manuscript, and we thank the American Cancer Society (RSG-07-035-01-CCG) and the National Institutes of Health (R01 CA124974 and R21 CA149774) for funding support.

REFERENCES

1. Wullschleger S, Loewith R, Hall MN. TOR signaling in growth and metabolism. *Cell.* 2006;124:471–484.
2. Ma XM, Blenis J. Molecular mechanisms of mTOR-mediated translational control. *Nat Rev Mol Cell Biol.* 2009;10:307–318.
3. Takai H, Wang RC, Takai KK, Yang H, de Lange T. Tel2 regulates the stability of PI3K-related protein kinases. *Cell.* 2007;131:1248–1259.
4. Mao JH, Kim IJ, Wu D, et al. FBXW7 targets mTOR for degradation and cooperates with PTEN in tumor suppression. *Science.* 2008;321:1499–1502.
5. Inoki K, Guan KL. Tuberous sclerosis complex, implication from a rare genetic disease to common cancer treatment. *Hum Mol Genet.* 2009;18(R1):R94–R100.
6. Chen J, Zheng XF, Brown EJ, Schreiber SL. Identification of an 11-kDa FKBP12-rapamycin-binding domain within the 289-kDa FKBP12-rapamycin-associated protein and characterization of a critical serine residue. *Proc Natl Acad Sci USA.* 1995;92:4947–4951.
7. Bai X, Ma D, Liu A, et al. Rheb activates mTOR by antagonizing its endogenous inhibitor, FKBP38. *Science.* 2007;318:977–980.
8. Sancak Y, Bar-Peled L, Zoncu R, Markhard AL, Nada S, Sabatini DM. Ragulator-Rag complex targets mTORC1 to the lysosomal surface and is necessary for its activation by amino acids. *Cell.* 2010;141:290–303.
9. Guertin DA, Stevens DM, Thoreen CC, et al. Ablation in mice of the mTORC components raptor, rictor, or mLST8 reveals that mTORC2 is required for signaling to Akt-FOXO and PKCalpha, but not S6K1. *Dev Cell.* 2006;11:859–871.
10. Copp J, Manning G, Hunter T. TORC-specific phosphorylation of mammalian target of rapamycin (mTOR): phospho-Ser2481 is a marker for intact mTOR signaling complex 2. *Cancer Res.* 2009;69:1821–1827.
11. Soliman GA, Acosta-Jaquez HA, Dunlop EA, et al. mTOR Ser-2481 autophosphorylation monitors mTORC-specific catalytic activity and clarifies rapamycin mechanism of action. *J Biol Chem.* 2010;285:7866–7879.
12. Julien LA, Carriere A, Moreau J, Roux PP. mTORC1-activated S6K1 phosphorylates Rictor on threonine 1135 and regulates mTORC2 signaling. *Mol Cell Biol.* 2010;30:908–921.
13. Chen CC, Jeon SM, Bhaskar PT, et al. FoxOs inhibit mTORC1 and activate Akt by inducing the expression of Sestrin3 and Rictor. *Dev Cell.* 2010;18:592–604.
14. Alexander A, Cai SL, Kim J, et al. ATM signals to TSC2 in the cytoplasm to regulate mTORC1 in response to ROS. *Proc Natl Acad Sci USA.* 2010;107:4153–4158.
15. Minami K, Tambe Y, Watanabe R, et al. Suppression of viral replication by stress-inducible GADD34 protein via the mammalian serine/threonine protein kinase mTOR pathway. *J Virol.* 2007;81:11106–11115.
16. Kuo HP, Lee DF, Chen CT, et al. ARD1 stabilization of TSC2 suppresses tumorigenesis through the mTOR signaling pathway. *Sci Signal.* 2010;3:ra9.
17. Costanzo-Garvey DL, Pfluger PT, Dougherty MK, et al. KSR2 is an essential regulator of AMP kinase, energy expenditure, and insulin sensitivity. *Cell Metab.* 2009;10:366–378.
18. Budanov AV, Karin M. p53 target genes sestrin1 and sestrin2 connect genotoxic stress and mTOR signaling. *Cell.* 2008;134:451–460.
19. Nogueira V, Park Y, Chen CC, et al. Akt determines replicative senescence and oxidative or oncogenic premature senescence and sensitizes cells to oxidative apoptosis. *Cancer Cell.* 2008;14:458–470.
20. Canto C, Jiang LQ, Deshmukh AS, et al. Interdependence of AMPK and SIRT1 for metabolic adaptation to fasting and exercise in skeletal muscle. *Cell Metab.* 2010;11:213–219.
21. Meric-Bernstam F, Gonzalez-Angulo AM. Targeting the mTOR signaling network for cancer therapy. *J Clin Oncol.* 2009;27:2278–2287.
22. Houghton PJ. Everolimus. *Clin Cancer Res.* 2010;16:1368–1372.
23. Shor B, Gibbons JJ, Abraham RT, Yu K. Targeting mTOR globally in cancer: thinking beyond rapamycin. *Cell Cycle.* 2009;8:3831–3837.
24. Kurmasheva RT, Dudkin L, Billups C, Debelenko LV, Morton CL, Houghton PJ. The insulin-like growth factor-1 receptor-targeting antibody, CP-751,871, suppresses tumor-derived VEGF and synergizes with rapamycin in models of childhood sarcoma. *Cancer Res.* 2009;69:7662–7671.
25. Aghajan M, Jonai N, Flick K, et al. Chemical genetics screen for enhancers of rapamycin identifies a specific inhibitor of an SCF family E3 ubiquitin ligase. *Nat Biotechnol.* 2010;28:738–742.
26. O'Reilly T, McSheehy PM. Biomarker development for the clinical activity of the mTOR inhibitor everolimus (RAD001): processes, limitations, and further proposals. *Transl Oncol.* 2010;3:65–79.
27. Phelps ME. Positron emission tomography provides molecular imaging of biological processes. *Proc Natl Acad Sci USA.* 2000;97:9226–9233.
28. Shields AF, Grierson JR, Kozawa SM, Zheng M. Development of labeled thymidine analogs for imaging tumor proliferation. *Nucl Med Biol.* 1996;23:17–22.
29. Wei LH, Su H, Hildebrandt IJ, Phelps ME, Czernin J, Weber WA. Changes in tumor metabolism as readout for mammalian target of rapamycin kinase inhibition by rapamycin in glioblastoma. *Clin Cancer Res.* 2008;14:3416–3426.
30. Aide N, Kinross K, Cullinane C, et al. ^{18}F-FLT PET as a surrogate marker of drug efficacy during mTOR inhibition by everolimus in a preclinical cisplatin-resistant ovarian tumor model. *J Nucl Med.* 2010;51:1559–1564.

Laboratory of Biopharmaceutical Research[1], National Institute of Biomedical Innovation; Laboratory of Toxicology and Safety Science[2], Graduate School of Pharmaceutical Sciences; The Center for Advanced Medical Engineering and Informatics[3]; Laboratory of Biomedical Innovation[4], Graduate School of Pharmaceutical Sciences, Osaka University, Osaka, Japan

Rho GDP-dissociation inhibitor alpha is associated with cancer metastasis in colon and prostate cancer

T. YAMASHITA[1,2,*], T. OKAMURA[1,*], K. NAGANO[1,*], S. IMAI[1], Y. ABE[1], H. NABESHI[1,2], T. YOSHIKAWA[1,2], Y. YOSHIOKA[1,2,3], H. KAMADA[1,3], Y. TSUTSUMI[1,2,3], S. TSUNODA[1,3,4]

Received July 7, 2011, accepted August 5, 2011

Shin-ichi Tsunoda, Ph.D, Laboratory of Biopharmaceutical Research, National Institute of Biomedical Innovation, 7-6-8 Saito-Asagi, Ibaraki, Osaka 567-0085, Japan.
tsunoda@nibio.go.jp
**These authors contributed equally to the work.*

Pharmazie 67: 253–255 (2012) *doi: 10.1691/ph.2012.1630*

Since metastasis is one of the most important prognostic factors in colorectal cancer, development of new methods to diagnose and prevent metastasis is highly desirable. However, the molecular mechanisms leading to the metastatic phenotype have not been well elucidated. In this study, a proteomics-based search was carried out for metastasis-related proteins in colorectal cancer by analyzing the differential expression of proteins in primary versus metastasis focus-derived colorectal tumor cells. Protein expression profiles were determined using a tissue microarray (TMA), and the results identified Rho GDP-dissociation inhibitor alpha (Rho GDI) as a metastasis-related protein in colon and prostate cancer patients. Consequently, Rho GDI may be useful as a diagnostic biomarker and/or a therapeutic to prevent colon and prostate cancer metastasis.

1. Introduction

Colorectal cancer is known as a major metastatic cancer, and 40–50% of patients already have a metastatic focus at presentation. Moreover, the 5-year survival of these patients is under 10% (Davies et al. 2005). Thus, metastasis is one of the most important prognostic factors in colorectal cancer. In order to improve rates of cancer remission, it will be necessary to clarify the detailed molecular mechanisms of cancer metastasis and to utilize this information to establish new diagnostic and therapeutic techniques. Many researchers have searched for metastasis-related molecules (Liu et al. 2010; Shuehara et al. 2011) using proteomics techniques (Hanash 2003). Comprehensive mapping of the molecular changes during metastasis would greatly improve our understanding of the recurrence and management of cancer. However, the knowledge gained so far in these studies has not been sufficient to improve cancer remission rates.

Here we show the potential of Rho GDI as a metastasis-related protein in colon and prostate cancer patients. In order to identify metastasis-related proteins, the protein expression patterns of human colorectal cancer cells with different metastatic characters were compared. Because these cells were derived from the same patient (SW480: a surgical specimen of a primary colon adenocarcinoma, SW620: a lymph node metastatic focus), cancer metastasis-related protein candidates could be effectively sought without background variations due to differences between individuals. Furthermore, by analyzing the expression of candidate proteins in many clinical samples using a TMA, we attempted to validate the association of these candidates with metastasis. TMA is a slide glass containing many clinical tissues, and it enables one to carry out a high-throughput analysis by evaluating the relationship between expression profiles of each candidate molecule and clinical information such as metastasis. (Imai et al. 2011; Yoshida et al. 2011).

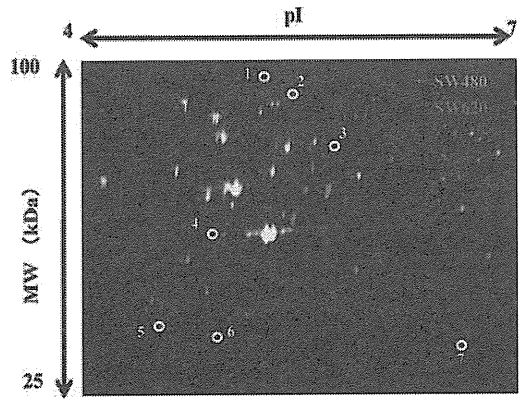

Fig. 1: 2D-DIGE image of fluorescently-labeled proteins from different metastatic human colorectal cancer cells. SW480 is human colorectal cancer cell line derived from a primary tumor and SW620 is derived from a metastatic focus from the same patient. Proteins from the colon cancer cells (SW480, SW620) were labeled with Cy3 and Cy5 respectively, and analyzed by 2D electrophoresis. The differentially-expressed spots (white circles) were then identified by LC-UHR TOF/MS

Table 1: High expression proteins in SW620 compared to SW480

	Accession	Protein name	MW (kDa)	pI	Ratio (SW620 / SW480)
1	P12109	collagen alpha-1(VI) chain	108.6	5.3	1.53
2	Q15459	splicing factor 3A subunit 1	88.9	5.2	1.61
3	P13797	T-plastin	70.9	5.5	1.59
4	P60709	actin cytoplasmic 1	42.1	5.3	1.50
5	P63104	14-3-3 zeta/delta	27.9	4.7	1.63
6	P52565	Rho GDP-dissociation inhibitor 1 (Rho GDI)	23.3	5.0	1.90
7	P30041	Peroxiredoxin-6 (PRDX6)	25.1	6.0	1.86

2. Investigations, results and discussion

In order to search for metastasis-related proteins, we analyzed differentially-expressed proteins between SW480 and SW620 by two-dimensional differential in-gel electrophoresis (2D-DIGE) (Fig. 1). As a result, 7 spots with at least a 1.5-fold-altered expression level were found by quantitative analysis, and these spots were identified by mass spectrometry (Table 1). Three molecules having a high SW620/SW480 expression ratio indicating a strong association with cancer metastasis were identified: Rho GDP-dissociation inhibitor alpha (Rho GDI), peroxiredoxin-6 (PRDX6) and 14-3-3 zeta/delta.

The expression profiles of these proteins were analyzed by immunohistochemistry using the TMA with colon cancer and multiple cancer tissues. Results of this analysis indicated that expression of PRDX6 and 14–3-3 zeta/delta had no relationship to the clinical status of cancer metastasis (data not shown). On the other hand, in positive cases of lymph node metastasis, the expression ratio of Rho GDI was significantly higher than in the negative cases. Furthermore, the same trend was seen when tissues from prostate cancer patients were analyzed (Table 2).

To confirm these results, the expression levels of Rho GDI protein in colon cancer cell lines with different metastatic potential (SW480 < SW620 < SW620-OK1 < SW620-OK2: Characteristics of SW620-OK1 and SW620-OK2 are described in *Experimental*) were investigated by western blot analysis (Fig. 2). The expression of Rho GDI was found to be up-regulated with the development of metastatic characteristics. These results suggested that Rho GDI is correlated with cancer metastasis.

Rho GDI has been identified as key regulator of Rho family GTPases. Activation of growth factor receptors and integrins can promote the exchange of GDP for GTP on Rho proteins (Bishop et al. 2000). Furthermore, GTP-bound Rho proteins interact with a range of effector molecules to modulate their activity or localization, and this leads to changes in cell behavior. It is clear that Rho family GTPases are involved in the control of cell morphology and motility (Etienne-Manneville et al. 2002; Hall et al. 1997; Van Aelst et al. 1997). The importance of Rho protein and Rho GDI in cancer progression, particularly in the area of metastasis, is becoming increasingly evident. Recently, some reports have indicated that the expression of Rho GDI was correlated with colorectal and breast cancer metastasis (Zhao et al. 2008; Kang et al. 2010). Thus, our findings are consistent with these reports and further suggest that the expression of Rho GDI is also correlated with prostate cancer metastasis. Consequently, Rho GDI should be considered as a diagnostic marker or new therapeutic target for cancer metastasis.

3. Experimental

3.1. Cell lines

SW480 is a human colorectal cancer cell line derived from a primary focus and SW620 is derived from a metastatic focus of the same patient. These cells were purchased from American Type Culture Collection and maintained at 37 °C using Leibovitz's L-15 medium (Wako) supplemented with 10% FCS. SW620-OK1 and -OK2 were established by the following procedure: 1×10^6 SW620 cells were injected into the spleens of nu/nu mice. After 8 weeks, SW620-OK1 was established from a liver metastatic focus. Furthermore, SW620-OK2 was established from SW620-OK1 using the same procedures.

3.2. 2D-DIGE analysis

Cell lysates were prepared from SW480 and SW620 and then solubilized with 7 M urea, 2 M thiourea, 4% CHAPS and 10 mM Tris-HCl (pH 8.5). The lysates were labeled at the ratio of 50 μg proteins: 400 pmol Cy3 or Cy5 protein-labeling dye (GE Healthcare Biosciences) in dimethylformamide according to the manufacturer's protocol. Briefly, the labelled samples were mixed with rehydration buffer (7 M urea, 2 M thiourea, 4% CHAPS, 2% DTT, 2% Pharmalyte (GE Healthcare Biosciences)) and applied to a 24-cm immobilized pH gradient gel strip (IPG-strip pH 4–7 NL) for separation in the first dimension. Samples for the spot-picking gel were prepared without labelling by Cy-dyes. For the second dimension separation, the IPG-strips were applied to SDS-PAGE gels (10% polyacrylamide and 2.7% N,N'-diallyltartardiamide gels). After electrophoresis, the gels were scanned with a laser fluoroimager (Typhoon Trio, GE Healthcare Biosciences). The spot-picking gel was scanned after staining with Deep Purple Total Protein Stain (GE Healthcare Biosciences). Quantitative analysis of protein spots was carried out with Decyder-DIA software (GE Healthcare Biosciences). For the antigen spots of interest, spots of 1 mm × 1 mm in size were picked using Ettan Spot Picker (GE Healthcare Biosciences).

3.3. In-gel tryptic digestion

Picked gel pieces were digested with trypsin as described below. The gel pieces were destained with 50% acetonitrile/50 mM NH_4HCO_3 for 20 min twice, dehydrated with 75% acetonitrile for 20 min, and then dried using a centrifugal concentrator. Next, 5 μl of 20 μl/ml trypsin (Promega) solution was added to each gel piece and incubated for 16 h at 37 °C. Three solutions were used to extract the resulting peptide mixtures from the gel pieces. First, 50 μl of 50% (v/v) acetonitrile in 0.1% (v/v) formic acid (FA) was added to the gel pieces, which were then sonicated for 5 min. Next, we collected the solution and added 80% (v/v) acetonitrile in 0.1% FA. Finally, 100% acetonitrile was added for the last extraction. The peptides were dried and then re-suspended in 10 μl of 0.1% FA.

3.4. Mass spectrometry and database search

Extracted peptides were analyzed by liquid chromatography Ultra High Resolution time-of-flight mass spectrometry (LC-UHR TOF/MS; maXis, Bruker Daltonics). The Mascot search engine (http://www.matrixscience.com) was initially used to query the entire theoretical tryptic peptide database as well as SwissProt (http://www.expasy.org/, a public domain database pro-

Table 2: Expression profile of Rho GDI in primary cancers with or without lymph node metastasis

	Number of Rho GDI positive cases (positive ratio)	
	in metastasis negative cases	in metastasis positive cases
Colon cancer*	11/14 (79%)	19/19 (100%)
Prostate cancer*	18/23 (78%)	11/11 (100%)

* $p < 0.05$: Mann Whitney U test

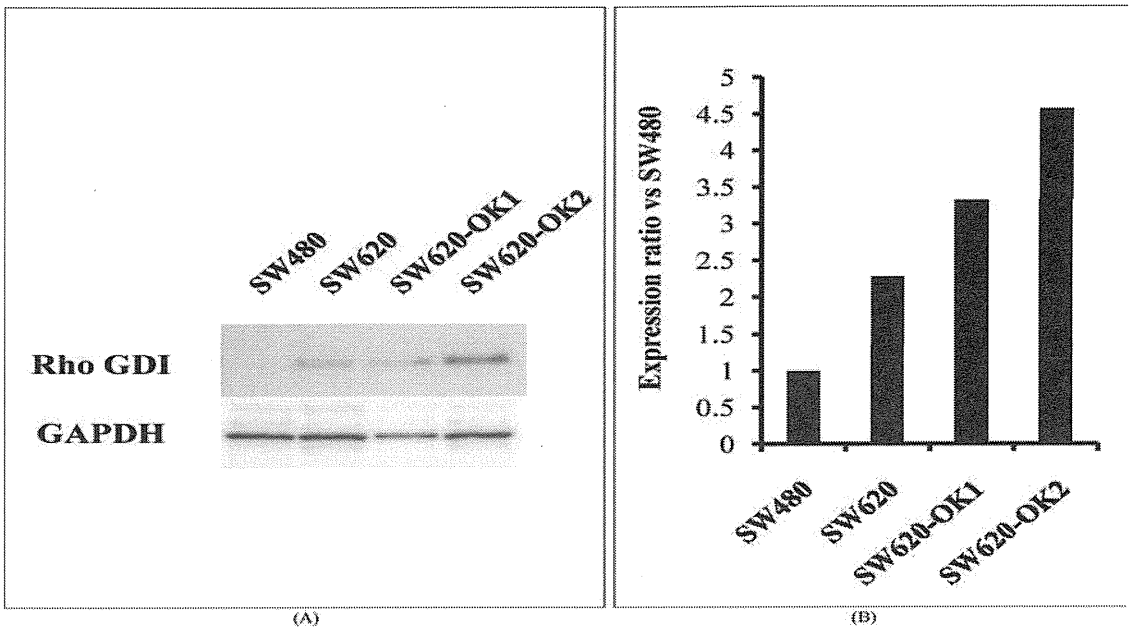

Fig. 2: Rho GDI expression levels in colon cancer cell lines with different metastatic abilities. Rho GDI expression levels in colon cancer cell lines (SW480, SW620, SW620-OK1, SW620-OK2) analyzed by western blotting (A). SW620-OK1, SW620-OK2 have been established as high metastatic sub-lines of SW620 using a mouse metastasis model. Intensity of the western blotting images was quantified by densitometry (B)

vided by the Swiss Institute of Bioinformatics). The search query assumed the following: (i) the peptides were monoisotopic (ii) methionine residues may be oxidized (iii) all cysteines are modified with iodoacetamide.

3.5. TMA Immunochemical staining

TMA slides with human colon cancer samples or multiple cancer samples (Biomax) were de-paraffinated in xylene and rehydrated in a graded series of ethanol washes. Heat-induced epitope retrieval was performed while maintaining the Target Retrieval Solution pH 9 (Dako) at the desired temperature according to manufacturer's instructions. After the treatment, endogenous peroxidase was blocked with 0.3% H_2O_2 in Tris-buffer saline (TBS) for 5 min. After washing twice with TBS, TMA slides were incubated with 10% BSA blocking solution for 30 min. The slides were then incubated with the anti-Rho GDI (Santa Cruz Biotechnology) for 60 min. After washing three times with wash buffer (Dako), each series of sections was incubated for 30 min with Envision + Dual Link (Dako). The reaction products were rinsed twice with wash buffer and then developed in liquid 3, 3'-diaminobenzidine (Dako) for 3 min. After the development, sections were counterstained with Mayer's hematoxylin. All procedures were performed using AutoStainer (Dako).

3.6. TMA Immunohistochemistry scoring

The optimized staining conditions for TMAs corresponding to human colon as well as multiple cancers were determined based on the co-existence of both positive and negative cells in the same tissue sample. Signals were considered positive when reaction products were localized in the expected cellular component. The criteria for scoring of stained tissues were as follows: the distribution score was 0 (0%), 1 (1–50%) or 2 (51–100%), indicating the percentage of positive cells among all tumor cells present in one tissue. The intensity of the signal (intensity score) was scored as 0 (no signal), 1 (weak), 2 (moderate) or 3 (marked). The distribution and intensity scores were then summed into a total score (TS) of TS0 (sum = 0), TS1 (sum = 2), TS2 (sum = 3), and TS3 (sum = 4–5). Throughout this study, TS0 or TS1 was regarded as negative, whereas TS2 or TS3 were regarded as positive.

3.7. Western Blot

Expression of Rho GDI in colon cancer cells was detected by anti-Rho GDI (Santa Cruz Biotechnology) and HRP conjugated anti-mouse IgG antibody (Sigma) using the ECL-plus system. Equal amounts of protein loading were confirmed by parallel β-actin immunoblotting, and signal quantification was performed by densitometric scanning.

Acknowledgements: This study was supported in part by Grants-in-Aid for Scientific Research from the Ministry of Education, Culture, Sports, Science and Technology of Japan, and from the Japan Society for the Promotion of Science (JSPS). This study was also supported in part by Health Labor Sciences Research Grants from the Ministry of Health, Labor and Welfare of Japan.

References

Bishop AL, Hall A (2000) Rho GTPases and their effector proteins. Biochem J 348: 241–255.

Davies RJ, Miller R, Coleman N (2005) Colorectal cancer screening: prospects for molecular stool analysis. Nat Rev Cancer 5: 199–209.

Etienne-Manneville S, Hall A (2002) Rho GTPases in cell biology. Nature 420: 629–635.

Hall A (1997). Rho GTPases and the Actin cytoskeleton. Science 279: 509–514.

Hanash S (2003) Disease proteomics. Nature 422: 226–232.

Imai S, Nagano K, Yoshida Y, Okamura T, Yamashita T, Abe Y, Yoshikawa T, Yoshioka Y, Kamada H, Mukai Y, Nakagawa S, Tsutsumi Y, Tsunoda S (2011). Development of an antibody proteomics system using a phage antibody library for efficient screening of biomarker proteins. Biomaterials 32: 162–169.

Kang S, Kim MJ, An H, Kim BG, Choi YP, Kang KS, Gao MQ, Park H, Na HJ, Kim HK, Yun HR, Kim DS, Cho NH (2010) Proteomic molecular portrait of interface zone in breast cancer. J Proteome Res 9: 5638–5645.

Liu R, Wang K, Yuan K, Wei Y, Huang C (2010) Integrative oncoproteomics strategies for anticancer drug discovery. Expert Rev Proteomics 7: 411–429.

Sahai E (2007). Illuminating the metastatic process. Nat Rev Cancer 7: 737–749.

Suehara Y, Tochigi N, Kubota D, Kikuta K, Nakayama R, Seki K, Yoshida A, Ichikawa H, Hasegawa T, Kaneko K, Chuman H, Beppu Y, Kawai A, Kondo T (2011) Secernin-1 as a novel prognostic biomarker candidate of synovial sarcoma revealed by proteomics. J Proteomics 74: 829–842.

Van Aelst L, D'Souza-Schorey C (1997) Rho GTPases and signaling networks. Genes Dev 11: 2295–2322.

Yoshida Y, Yamashita T, Nagano K, Imai S, Nabeshi H, Yoshikawa T, Yoshioka Y, Abe Y, Kamada H, Tsutsumi Y, Tsunoda S (2011) Limited expression of reticulocalbin-1 in lymphatic endothelial cells in lung tumor but not in normal lung. Biochem Biophys Res Commun 405: 610–614.

Zhao L, Wang H, Li J, Liu Y, Ding Y (2008) Overexpression of Rho GDP-dissociation inhibitor alpha is associated with tumor progression and poor prognosis of colorectal cancer. J Proteome Res 7: 3994–4003.

—Review—

抗体工学を駆使した創薬ターゲットの探索技術

鎌田春彦

Exploring Technique for Pharmaceutical Target Using Antibody Technology

Haruhiko Kamada

Laboratory of Biopharmaceutical Research, National Institute of Biomedical Innovation; 7-6-8 Saito-Asagi, Ibaraki, Osaka 567-0085, Japan.

(Received December 2, 2011)

A monoclonal antibody (Mab), due to its specific binding ability to a target protein, can potentially be one of the most useful tools for the functional analysis of proteins in recent proteomics-based research. However, the production of Mab is a very time-consuming and laborious process (*i.e.*, preparation of recombinant antigens, immunization of animals, preparation of hybridomas), making it the rate-limiting step in using Mabs in high-throughput proteomics research, which heavily relies on comprehensive and rapid methods. Therefore, there is a great demand for new methods to efficiently generate Mabs against a group of proteins identified by proteome analysis. Here, we describe a useful method called "Antibody proteomic technique" for the rapid generations of Mabs to pharmaceutical target, which were identified by proteomic analyses of disease samples (ex. tumor tissue, *etc.*). We also introduce another method to find profitable targets on vasculature, which is called "Vascular proteomic technique". Our results suggest that this method for the rapid generation of Mabs to proteins may be very useful in proteomics-based research as well as in clinical applications.

Key words——monoclonal antibody; proteomics; biomarker; biologics

1. はじめに

近年，ゲノム解析やジーンチップ解析などのオミクス研究の進展に伴い，バイオマーカー探索や創薬のための標的分子の探索が盛んに行われている.[1,2] このような医薬品開発に資する標的分子の探索は，画期的な医薬品を開発する上で最も重要なステップであり，探索の結果から得られた標的分子に作用する薬物は，これまで治療法のなかった疾患の治療に貢献すると考えられている．このような疾患の発症や悪化の原因となる標的分子の探索のうち，とりわけプロテオミクスを用いたタンパク質の発現解析は注目を集めており，医薬品の開発に貢献するものと期待されている.[3] しかしながら，上述したオミクス解析全般に言えることであるが，標的分子の探索から創薬ターゲットの発見につながった例はこれまでほとんどないのが現状である．疾患の発症や悪化に連動して発現変化が認められる疾患関連分子は，病態時に数百以上のオーダーで発現変動しており，そのほとんどが疾患の発症や悪化には直接関係していないものであるとされている.[4] したがって，画期的診断法・治療法を開発していくためには，このような疾患関連分子の中から，創薬に資する分子を効率よく同定する必要があり，これまで用いられてきた方法をより進歩させた新しい探索法の開発に期待が寄せられている.

このように標的分子を検出したり薬理効果発現を評価したりするためには，標的分子を認識可能なプローブが必要であり，標的分子候補タンパク質に結合活性を持つ抗体の開発がますます重要視されつつある．特に，最近では抗体そのものを医薬品化した抗体医薬品がリウマチやがんなど様々な難治性疾患に臨床応用され，バイオ医薬品の市場規模が急拡大している.[5] これまでに臨床応用された抗体医薬品としては抗サイトカイン抗体などの活性中和抗体や細胞表面のマーカー分子を認識する抗細胞抗体がほ

独立行政法人医薬基盤研究所バイオ創薬プロジェクト（〒567-0085 大阪府茨木市彩都あさぎ 7-6-8）
e-mail: kamada@nibio.go.jp

本総説は，日本薬学会第 131 年会シンポジウム S16 で発表したものを中心に記述したものである.

とんどであるが，最近では受容体に結合して活性を示すアゴニスト抗体や2種類のマーカー分子を認識して活性を示すバイスペシフィック抗体なども臨床応用に向けた検討が進められつつある.[6]

このような抗体医薬は，従来の低分子医薬品や分子プローブでは困難な疾患に対する治療や診断が可能であるために，様々な難治性疾患の克服に向け大いに利用されつつあるところであるが，抗体医薬の開発を効率よく進めるためにはいくつかの問題点があることが知られている．その1つの問題点として，一般的に1種類の抗体の作製期間は，数ヵ月程度必要とされ，このことが原因となって標的分子が同定されてからその評価までには大きなタイムラグが生じており，タンパク質の中からスクリーニングする上での障害となっていることが指摘されている.

もし数多くの発現変動タンパク質に対する特異的抗体が一挙かつ迅速に作製できれば，定量解析（ELISA, Western blot（WB), *etc.*），局在解析（免疫染色，WB, *etc.*），機能解析（細胞増殖活性，細胞分化解析，*etc.*）が可能になり，タンパク質の発現挙動と疾患の発症・悪化などとの連関解析が格段に進展するものと考えられる．そこでわれわれは，プロテオーム解析技術の最適化とともに，数多くの変動タンパク質の中から，創薬に向けて標的分子を絞り込む基盤技術の開発を行うために，プロテオミクスと抗体工学を融合させた新しい「抗体プロテオミクス技術」を開発した．本総説では，この「抗体プロテオミクス技術」を概説し創薬ターゲット候補分子の同定に至った例を示すとともに，抗体をバイオ医薬品として利用する際に有用な探索技術として「血管プロテオミクス」に関してもその研究成果を一部紹介する.

2. 抗体プロオミクス技術

抗体は生体内で外来異物由来のタンパク質抗原を認識し，それを捕捉するための生体防御分子としての役割を持っている．すなわち，あらゆる外来抗原に対して，結合可能なレパートリーを有するタンパク分子群である．その性質を利用し，古くからタンパク質の定性や定量のためのツールとして，生命科学の分野で活用されている．われわれは，この抗体の持つ性質に着目し，生体の抗体レパートリーを再現した抗体ライブラリを手に持つことで，抗原に結合可能な抗体分子を短時間で手に入れたいと考えた．この膨大な抗体ライブラリの中から目的の抗体を迅速に単離するための基盤技術としてわれわれはファージ抗体ライブラリに着目した．このファージ抗体ライブラリは，抗体の抗原認識部位にあたるV領域をリンカーで結んだ一本鎖抗体（scFV抗体）をファージの外殻タンパク質gⅢとの融合タンパク質としてファージ表面に提示しており，ファージウイルスの表面に提示させた一本鎖抗体をライブラリとして作製することが可能である.[7] この技術は，一般的に用いられるハイブリドーマ法とは異なり，*in vitro* のセレクションのみで迅速にモノクローナル抗体を単離することができ，2週間程度の短期間でモノクローナル抗体が得られる方法である．この技術を従来から知られる二次元電気泳動法などを利用したプロテオミクス技術と組み合わせ，単離・精製したタンパク質に対して上述した抗体ライブラリからの抗体の単離を行おうと考えた．さらに得られた抗体を利用し，免疫染色を利用した抗原の発現解析を組織マイクロアレイを用いて迅速に行うことにした．この組織マイクロアレイは，がんなどの疾患組織が直径1–2 mm程度の組織片として添付されたスライドガラスであり，一挙に100症例以上もの組織を免疫染色などで検出することが可能である.[8] この組織マイクロアレイを用いることで，これまで発現解析が困難であった組織を一挙に染色でき，極めて短時間にタンパク質の発現状態を知ることができる．この抗体ライブラリをプロテオミクス，さらに組織マイクロアレイと融合した「抗体プロテオミクス技術」をわれわれは独自に開発し，がんの標的分子の探索を行うことにした（Fig. 1）.[9]

まず，ナイーブファージ抗体ライブラリをウェスタンブロット等に用いられるメンブランに固相化した精製タンパク質に対してパンニングを行い，わずか10 ng程度のモデル抗原からでもモノクローナル抗体を得ることができた．さらに，この方法を乳がんの診断・治療に応用し，画期的な標的分子の探索を行うために，正常乳腺とのタンパク質比較解析を行った．その結果，十数種類前後の標的分子候補の中から最も有用な創薬ターゲットとしてEphrin Receptor A10（EphA10）と呼ばれる分子を同定した（Table 1）．この分子は，乳がん細胞に特異的に発現する上，既存の乳がんの標的分子として知られるHer-2よりも高い陽性率を示し，Her-2陰性患者

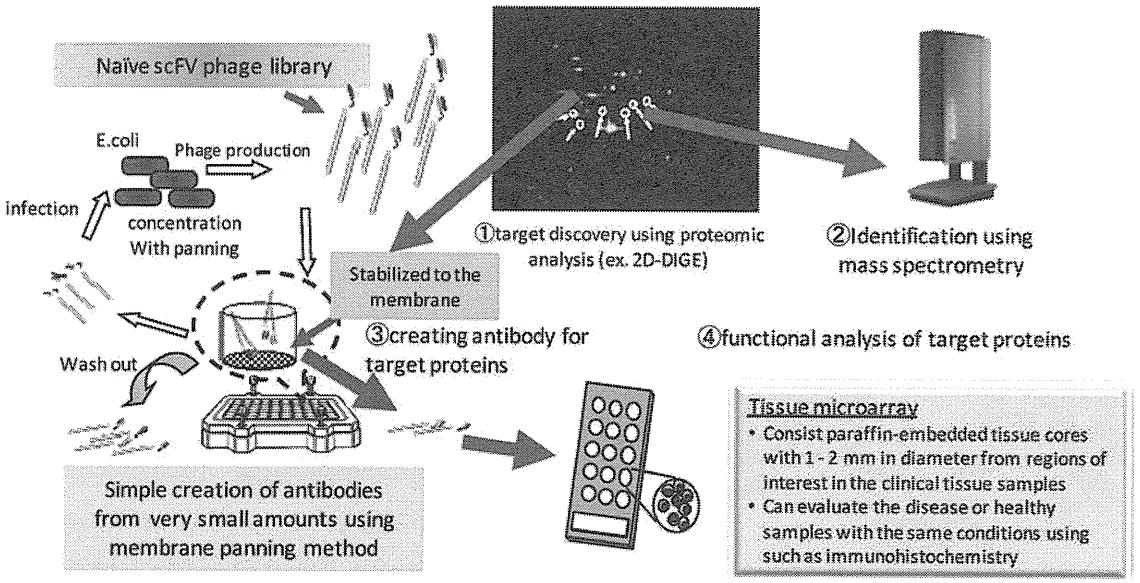

Fig. 1. Schematic Protocol of Antibody Proteomics

Table 1. Protein Expression of Identified Drug Target Candidates Using Tissue Microarray

Target candidate	Positive ratio	
	Healthy mammal	Breast cancer
Her2 (Control)	0/15(0%)	53/189(28%)
IkappaBR	3/15(20%)	22/189(12%)
SPATA5 protein	0/15(0%)	0/189(0%)
beta actin variant	0/15(0%)	0/189(0%)
TRAIL-R2	0/15(0%)	119/189(63%)
RREB-1	1/15(6%)	83/189(44%)
FLJ31438 protein	0/15(0%)	0/189(0%)
hPAK65	0/15(0%)	0/189(0%)
Cytokeratin 8	0/15(0%)	137/189(73%)
XRN1 protein	0/15(0%)	0/189(0%)
Jerky protein homolog-like	0/15(0%)	0/189(0%)
EPH receptor A10 (EphA10)	0/15(0%)	93/189(49%)

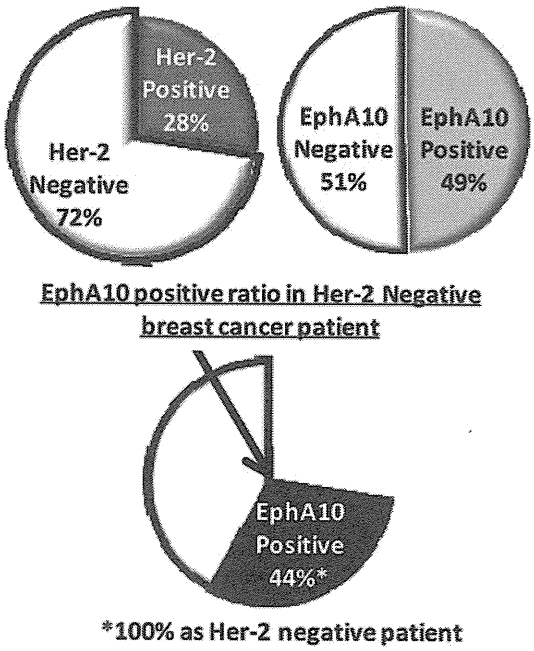

Fig. 2. EphA10 Expression in Breast Cancer Patients

の約半数に発現する創薬ターゲットとしても有用性の高い分子であることが明らかになった（Fig. 2）.

3. 血管プロテオミクス

このように創薬ターゲットとしての分子探索にプロテオミクスの手法を用いることは極めて有用であり，今後数多くの標的分子を発見できる可能性を示唆している．その一方で，現在の抗体医薬の標的分子のほとんどが，膜タンパク質及び分泌タンパク質を標的とした分子標的治療薬である事実からも，抗体医薬を用いる限り，現在の技術背景では，細胞質内に存在するタンパク質を標的にするのは数多くの問題点があると考えられている.[10] したがって，抗体医薬の開発を念頭に置く場合には，膜タンパク質や分泌タンパク質を標的にすることが実用化において最も近道であると考えられる．そこで，細胞膜タンパク質，及び細胞外マトリクス等の分泌タンパク質の発現挙動の解析のために，全身の血管をビオチン化試薬にてラベル化し，疾患組織にある血管内皮

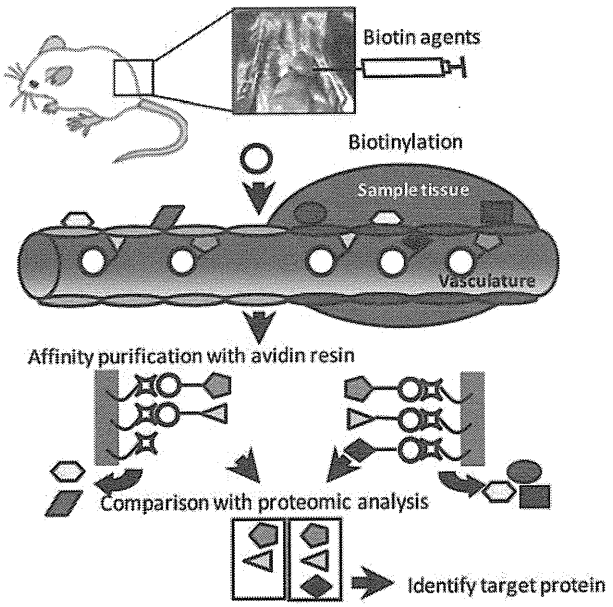

Fig. 3. Schematic Protocol of Vasculature Proteomics

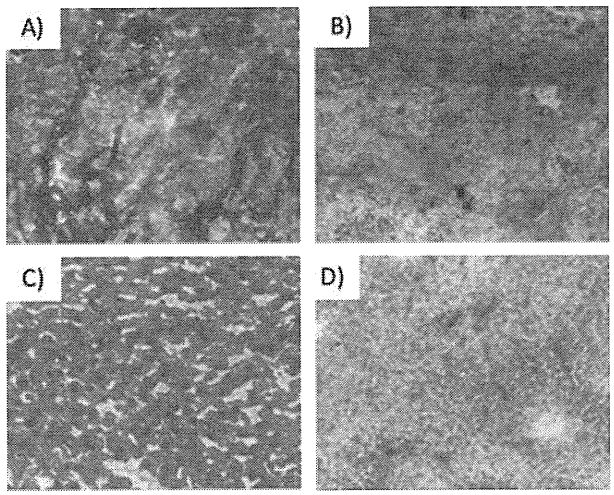

Fig. 4. BST-2 Expression in Metastatic Lymphoma

(A) Liver metastatic tumor; (B) Spleen metastatic tumor; (C) Normal liver; (D) Normal spleen. Immunohistochemistry were performed by using anti-BST-2 polyclonal antibody. Tumor vascular regions were stained (dark gray) but not normal tissues.

細胞の膜タンパク質並びに分泌タンパク質を効率よく回収・精製可能な *in vivo* biotinylation 法を活用し血管プロテオームを行うことにした.[11] Figure 3 にその概要を示す. この *in vivo* biotinylation 法は, 細胞膜タンパク質を解析する場合に, 現在汎用されている組織抽出後の膜タンパク質を回収する方法とは異なり, 直接組織細胞の外側からラベル化を行うため, 小胞膜のコンタミネーションのリスクを回避できる. 当然のことながら, 細胞外の膜タンパク質等を選択的にビオチンラベルするため, 解析結果から得られたタンパク質候補に対するモノクローナル抗体は, 通常の方法でプロテオーム解析して得られたタンパク質候補（多くの場合, シャペロンタンパク質やヒートショックタンパク質といった細胞内タンパク質）に対する抗体よりも, 基礎医学・臨床医学的な有用性に優れていることは言うまでもない. そのうえ, 血管側からビオチン化しているため, 組織中の血管内皮細胞がより効率よくラベル化されており, 抗体医薬の開発には極めて有用な方法であると考えられる.

この血管プロテオミクスを担がんマウスモデルに対して行い, 転移性リンパ腫の治療に向けた抗原の探索を行った.[12] 具体的には, 抗体のラベル化等に用いるビオチン化試薬を, *in vivo* に直接投与・環流することで, 組織に存在する血管を直接ラベル化した. その結果, 腫瘍血管での発現がこれまでにも報告されている Transferrin 受容体が同定された一方, これまで知られていなかった新しいがん血管関連抗原として BST-2 の発現を見い出した（Fig. 4）.[12] BST-2 は, 肝臓や脾臓に転移したリンパ腫の血管部位に特異的に発現しており, これを標的としたがん治療薬の開発が期待される. 実際に, この BST-2 に対する抗体を投与することで, 腫瘍の増殖が抑制される結果も見い出しており, 今後これらを利用した抗体医薬の開発も期待されるところである.

4. 結論と展望

抗体プロテオミクス技術はプロテオミクスと抗体工学の技術を組み合わせ, さらに組織マイクロアレイによるバリデーションを迅速に行うことで, 標的分子を迅速にバリデーションできる技術である. この技術により, これまで標的分子の探索から発現解析までの膨大な時間と労力を, わずか 2–3 週間程度の期間で達成できる極めて有用な技術として開発することができた. また先述したように血管プロテオミクスは, 個体レベルでのプロテオミクスを可能とするうえ, 細胞膜タンパク質及び細胞外マトリクス等の分泌タンパク質を効果的にラベル化できる方法であり, 細胞質内タンパク質のコンタミネーションを回避できるという圧倒的な利点を有している. この 2 つのプロテオミクス技術を融合することで, 疾患における創薬ターゲットの同定に留まらず, 新しい抗体医薬の開発法として利用することを考えてい

る．今後，本方法を用いて同定された抗原に対する抗体を作製することで，バイオマーカーの検出や評価に利用できるものと期待されるとともに，タンパク質の発現挙動解析，並びに同定作業を現在も進めているところであり，プロテオミクスによる解析基盤の確立に向けた開発・最適化を今後も行う予定である．

謝辞　本研究は，多くの共同研究者の先生方に御支援を賜りつつ，大阪大学薬学研究科毒性学分野及び医薬基盤研究所バイオ創薬プロジェクトのスタッフ・学生の皆さんとともに推進したものです．この場をお借りして，心より御礼を申し上げます．さらに，プロテオーム解析にあたり医薬基盤研究所免疫シグナルプロジェクト 世良田　聡先生，仲　哲治先生にご協力頂くとともに，血管プロテオミクスに関しては，スイス連邦工科大学チューリッヒ校(ETHZ)のダリオ・ネリ教授のご協力を得ました．また本研究の推進にあたり，厚生労働科学研究費補助金並びに文部科学研究費補助金の支援を賜りました．ここに深謝申し上げます．

REFERENCES

1) Kramer R., Cohen D., *Nat. Rev. Drug Discov.*, **3**, 965–972 (2004).
2) Butte A., *Nat. Rev. Drug Discov.*, **1**, 951–960 (2002).
3) Latterich M., Schnitzer J. E., *Nat. Biotechnol.*, **29**, 600–602 (2011).
4) Rifai N., Gillette M. A., Carr S. A., *Nat. Biotechnol.*, **24**, 971–983 (2006).
5) Goodman M., *Nat. Rev. Drug Discov.*, **8**, 837 (2009).
6) Nelson A. L., Reichert J. M., *Nat. Biotechnol.*, **27**, 331–337 (2009).
7) Yamashita T., Utoguchi N., Suzuki R., Nagano K., Tsunoda S., Tsutsumi Y., Maruyama K., *Yakugaku Zasshi*, **130**, 479–485 (2010).
8) Giltnane J. M., Rimm D. L., *Nat. Clin. Pract. Oncol.*, **1**, 104–111 (2004).
9) Imai S., Nagano K., Yoshida Y., Okamura T., Yamashita T., Abe Y., Yoshikawa T., Yoshioka Y., Kamada H., Mukai Y., Nakagawa S., Tsutsumi Y., Tsunoda S., *Biomaterials*, **32**, 162–169 (2011).
10) Williams B. R., Zhu Z., *Curr. Med. Chem.*, **13**, 1473–1480 (2006).
11) Roesli C., Neri D., *J. Proteomics*, **73**, 2219–2229 (2010).
12) Schliemann C., Roesli C., Kamada H., Borgia B., Fugmann T., Klapper W., Neri D., *Blood*, **115**, 736–744 (2010).

ORIGINAL ARTICLE

Serum Leucine-rich Alpha-2 Glycoprotein Is a Disease Activity Biomarker in Ulcerative Colitis

Satoshi Serada, PhD, Minoru Fujimoto, MD, PhD,* Fumitaka Terabe, MD, PhD,*† Hideki Iijima, MD, PhD,† Shinichiro Shinzaki, MD, PhD,† Shinya Matsuzaki, MD,‡ Tomoharu Ohkawara, MD,* Riichiro Nezu, MD, PhD,§ Sachiko Nakajima, MD, PhD,† Taku Kobayashi, MD, PhD,‖ Scott Eric Plevy, MD, PhD,‖ Tetsuo Takehara, MD, PhD,† and Tetsuji Naka, MD, PhD**

Background: Reliable biomarkers for monitoring disease activity have not been clinically established in ulcerative colitis (UC). This study aimed to investigate whether levels of serum leucine-rich alpha-2 glycoprotein (LRG), identified recently as a potential disease activity marker in Crohn's disease and rheumatoid arthritis, correlate with disease activity in UC.

Methods: Serum LRG concentrations were determined by enzyme-linked immunosorbent assay (ELISA) in patients with UC and healthy controls (HC) and were evaluated for correlation with disease activity. Expression of LRG in inflamed colonic tissues from patients with UC was analyzed by western blotting and immunohistochemistry. Interleukin (IL)-6-independent induction of LRG was investigated using IL-6-deficient mice by lipopolysaccharide (LPS)-mediated acute inflammation and dextran sodium sulfate (DSS)-induced colitis.

Results: Serum LRG concentrations were significantly elevated in active UC patients compared with patients in remission ($P < 0.0001$) and HC ($P < 0.0001$) and were correlated with disease activity in UC better than C-reactive protein (CRP). Expression of LRG was increased in inflamed colonic tissues in UC. Tumor necrosis factor alpha (TNF-α), IL-6, and IL-22, serum levels of which were elevated in patients with active UC, could induce LRG expression in COLO205 cells. Serum LRG levels were increased in IL-6-deficient mice with LPS-mediated acute inflammation and DSS-induced colitis.

Conclusions: Serum LRG concentrations correlate well with disease activity in UC. LRG induction is robust in inflamed colons and is likely to involve an IL-6-independent pathway. Serum LRG is thus a novel serum biomarker for monitoring disease activity in UC and is a promising surrogate for CRP.

(Inflamm Bowel Dis 2012;000:000–000)

Key Words: IBD, ulcerative colitis, biomarker, leucine-rich alpha-2 glycoprotein, DSS

The chronic inflammatory bowel diseases (IBDs), Crohn's disease (CD) and ulcerative colitis (UC), are typically characterized by episodes of acute flares and remission.[1,2] Depending on disease location and extent, exacerbation leads to diarrhea, abdominal pain, and systemic symptoms such as fatigue and weight loss.[3–5] Disease activity indices have been developed as outcome measures in clinical trials.[6,7] They may help to reproducibly and validly assess the patients' status and to support therapeutic decision-making.[6] Variables of disease activity indices comprise frequency of bowel movements, severity of abdominal pain, general well-being, occurrence of extraintestinal manifestations, and laboratory parameters.[8]

One of the most important protein biomarkers increased during the inflammatory state is C-reactive protein (CRP). However, elevation of serum CRP levels is not observed in certain inflammatory diseases. While serum CRP levels are highly increased in CD and rheumatoid arthritis (RA) patients and widely used for monitoring

Additional Supporting Information may be found in the online version of this article.

Received for publication February 12, 2012; Accepted February 13, 2012.

From the *Laboratory for Immune Signal, National Institute of Biomedical Innovation, Osaka, Japan, †Department of Gastroenterology and Hepatology, Osaka University Graduate School of Medicine, Osaka, Japan, ‡Department of Obstetrics and Gynecology, Osaka University Graduate School of Medicine, Osaka, Japan, §Department of Surgery, Osaka Rosai Hospital, Osaka, Japan, ‖Center for Gastrointestinal Biology and Diseases, University of North Carolina School of Medicine, Chapel Hill, North Carolina, USA.

Supported by the Grant-in-Aid for Scientific Research (C) (22591101) from the Japanese Ministry of Education, Science, Sports, and Culture; a grant-in-aid for the Program for Promotion of Fundamental Studies in Health Sciences of the National Institute of Biomedical Innovation and Grant-in-Aid from the Ministry of Health, Labour and Welfare of Japan.

Reprints: Tetsuji Naka, Laboratory for Immune Signal, National Institute of Biomedical Innovation, 7-6-8, Saito-asagi, Ibaraki, Osaka 567-0085, Japan (e-mail: tnaka@nibio.go.jp).

DOI 10.1002/ibd.22936

Published online in Wiley Online Library (wileyonlinelibrary.com).

TABLE 1. Characteristics of Patients with Ulcerative Colitis (UC)

Characteristics	Patients with UC	Patients with Appendicitis and Diverticulitis
Number (male:female)	82 (41:41)	17 (8:9)
Age, yr, mean (SD)	40.1 (15.7)	33.1 (13.7)
Age at diagnosis, yr, mean (SD)	34.7 (15.6)	33.1 (13.7)
Bowel surgery (including appendectomy), *N* (%)	7 (8.54)	
Treatment		
Salazosulfapyridine or mesalazine, N (%)	66 (80.5)	
Steroids, *N* (%)	16 (19.5)	
Immunomodulators, *N* (%)	3 (3.7)	
Disease location (*N*)		
Extensive colitis/left-sided colitis/proctitis	37/30/15	
CRP, mg/dL, mean (SD)	0.884 (1.967)	8.47 (7.69)
WBC cells/μl, mean (SD)	6716 (2317)	12307 (3603)
CAI, mean (SD)	4.71 (4.89)	
Matts's score, mean (SD)	2.27 (0.89)	

disease activity, only modest to absent CRP responses are observed in systemic lupus erythematosus (SLE), dermatomyositis, Sjogren's syndrome, or UC, although active inflammation is present.[9–11] In UC, endoscopic disease activity may predict future clinical symptoms,[12] but direct endoscopic or radiologic visualization of the degree of inflammation is rarely performed in outpatients with inactive or mild disease. Therefore, alternative biomarkers, which can conveniently and precisely monitor disease activity during therapy in inflammatory diseases, are required for the determination of adequate treatment.

By using a quantitative proteomic approach, we have previously reported that serum levels of leucine-rich alpha-2 glycoprotein (LRG) were elevated in patients with active RA and serum LRG levels were correlated with disease activity of not only RA but also CD, suggesting that serum LRG is a serological biomarker for monitoring disease activity.[13] LRG is an ≈50 kDa glycoprotein and contains repetitive sequences with a leucine-rich motif, first purified from human serum.[14,15] LRG has been reported to be expressed by the liver cells and neutrophils[16,17]; however, its function remains unclear. To date, the relationship between serum LRG levels and disease activity in UC has not been assessed. In this study we investigated serum LRG expression levels in UC patients and evaluated their correlation with clinical disease activity. Serum LRG levels were significantly increased in the active UC patients. LRG expression was upregulated in the inflamed colonic mucosa of UC possibly through stimulation by various cytokines including tumor necrosis factor alpha (TNF-α), interleukin (IL)-6, and IL-22, the expression of which are increased in active UC. Moreover, we show that serum LRG correlates more strongly than CRP with disease activity in UC. Therefore, serum LRG may be a useful disease activity biomarker for UC.

MATERIALS AND METHODS

Patients and Sera

Sera were obtained from patients with UC ($n = 82$), appendicitis ($n = 13$), and diverticulitis ($n = 4$) and surgical or biopsy samples were obtained from patients with UC ($n = 10$) from Osaka University Hospital (Osaka, Japan) and the Department of Surgery, Osaka Rosai Hospital, respectively. Sera from healthy controls (HCs) ($n = 50$), age/sex-matched with UC patients, were used. Diagnosis of UC was based on conventional clinical, radiological, endoscopic, and histopathological criteria. Clinical activities were determined using the Clinical Activity Index (CAI) for UC.[18] Clinical remission was defined as CAI <6.[19] In addition to CAI, the endoscopic findings were also graded according to Matts' criteria.[20] Endoscopic remission was defined as Matts' score ≤ 2. Detailed patient characteristics are presented in Table 1. For Caucasian patients with UC, sera ($n = 30$) were obtained from the Department of Medicine, University of North Carolina Hospital (Chapel Hill, NC). Sera from HCs ($n = 19$), age/sex-matched with UC patients, were used. Detailed patient characteristics are presented in Table 2, while data of disease activity of UC is not available.

Quantification of Serum LRG and Cytokines

Human serum LRG and mouse serum LRG were quantitated by human LRG assay kit (IBL, Fujioka, Japan) and mouse LRG assay kit (IBL, Fujioka, Japan). These enzyme-linked immunosorbent assay (ELISA) assays were performed